Leading with morphometric data in fossil vertebrates: a case-study of the intra-specific variation and allometry of the skull of Late Cretaceous side-necked turtle *Bauruemys elegans* (Pleurodira, Podocnemididae) (#11125)

First submission

Please read the **Important notes** below, and the **Review guidance** on the next page.
When ready **submit online**. The manuscript starts on page 3.

Important notes

Editor and deadline
Laura Wilson / 20 Jun 2016

Files	9 Figure file(s) 4 Table file(s) 5 Raw data file(s) Please visit the overview page to **download and review** the files not included in this review pdf.
Declarations	No notable declarations are present

Review guidelines

Please in full read before you begin

How to review

When ready **submit your review online**. The review form is divided into 5 sections. Please consider these when composing your review:

1. **BASIC REPORTING**
2. **EXPERIMENTAL DESIGN**
3. **VALIDITY OF THE FINDINGS**
4. General comments
5. Confidential notes to the editor

You can also annotate this **pdf** and upload it as part of your review

To finish, enter your editorial recommendation (accept, revise or reject) and submit.

BASIC REPORTING

- Clear, unambiguous, professional English language used throughout.
- Intro & background to show context. Literature well referenced & relevant.
- Structure conforms to **PeerJ standard**, discipline norm, or improved for clarity.
- Figures are relevant, high quality, well labelled & described.
- Raw data supplied (See **PeerJ policy**).

EXPERIMENTAL DESIGN

- Original primary research within **Scope of the journal**.
- Research question well defined, relevant & meaningful. It is stated how research fills an identified knowledge gap.
- Rigorous investigation performed to a high technical & ethical standard.
- Methods described with sufficient detail & information to replicate.

VALIDITY OF THE FINDINGS

- Impact and novelty not assessed. Negative/inconclusive results accepted. *Meaningful* replication encouraged where rationale & benefit to literature is clearly stated.
- Data is robust, statistically sound, & controlled.
- Conclusion well stated, linked to original research question & limited to supporting results.
- Speculation is welcome, but should be identified as such.

The above is the editorial criteria summary. To view in full visit **https://peerj.com/about/editorial-criteria/**

Leading with morphometric data in fossil vertebrates: a case-study of the intra-specific variation and allometry of the skull of Late Cretaceous side-necked turtle *Bauruemys elegans* (Pleurodira, Podocnemididae)

Thiago F. Mariani Corresp., [1] , **Pedro S. R. Romano** [1]

[1] Deparatamento de Biologia Animal, Universidade Federal de Viçosa, Viçosa, MG, Brazil

Corresponding Author: Thiago F. Mariani
Email address: tmariani.bio@gmail.com

Background. Previous quantitative studies about *Bauruemys elegans* (Suárez, 1969) shell variation, as well as the taphonomy interpretation of its type locality, have suggested that all specimens collected in this locality may have belonged to the same population. We rely on this hypothesis in a morphometric study of the skull. Also, we tried to assess the eating preference habits differentiation that might be explained as due to ontogenetic changes. **Methods.** We carried out an ANOVA comparing 29 linear measurements from 21 skulls of *B. elegans* using both caliper and ImageJ. A Principal Components Analysis (PCA) was performed using 27 measurements (excluding total length and width characters) in order to visualize patterns of scattering based on the form variance. Then, a PCA was carried out using ratios of length and width of each original measurement to assess shape variation among individuals. Finally, original measurements were log-transformed to describe allometries along ontogeny. **Results.** No statistical differences were found between caliper and ImageJ measurements. The first three PCs of the first analysis comprising 70.2% of the variance. PC1 was related to size variation and all others related to shape variation. Two specimens have been plotted outside the 95% ellipse in PC1xPC2 axes. The first three PCs of the second PCA comprised 64% of the variance. When considering PC1xPC2, all specimens have been plotted inside the 95% ellipse. In the third analysis, five measurements were positively allometric, 18 were negatively allometric and four represent truly negatively allometry. All bones of the posterior and the lateral emarginations, as well as the squamosal, lengthen due to size increasing, different from the jugal and the quadratojugal which decrease in width. **Discussion.** ImageJ is useful in replacing caliper since there was no statistical differences. Yet, iterative imputation is more appropriate to deal with missing data in PCA. Some specimens show small differences in form and shape. Form differences were interpreted as due to ontogeny, whereas shape differences are related to feeding changes along growth. Moreover, all

outlier specimens are crushed and/or distorted, thus the form/shape differences might be partially due to taphonomy. The allometric lengthen of parietal, quadrate, squamosal, maxilla, associated with the narrowing of jugal and quadratojugal may be related to changes in feeding habit between different stages of development. This change in shape might represent a progressive skull stretching and enlargement of posterior and lateral emargination during ontogeny, and consequently, the increment of the feeding-*apparatus* musculature. Smaller individuals may have fed of softer diet whereas bigger ones probably have had a harder diet, as seen in some living species of *Podocnemis*. We conclude that the skull variation is higher than expected and might be related to differences in feeding habits along the ontogeny of *B. elegans*.

Leading with morphometric data in fossil vertebrates: a case-study of the intra-specific variation and allometry of the skull of Late Cretaceous side-necked turtle *Bauruemys elegans* (Pleurodira, Podocnemididae)

Thiago Fiorillo Mariani[1], Pedro Seyferth R. Romano[1]

[1] Departamento de Biologia Animal, Universidade Federal de Viçosa, Viçosa, Minas Gerais, Brazil.

Corresponding author:

Thiago Mariani[1]

Av. P. H. Rolfs, Anexo do Centro de Ciências Biológias II, Third Floor, Room 305, Viçosa, Minas Gerais, 36570-900, Brazil

Email address: tmariani.bio@gmail.com

19

20

21 1. Introduction

22 1.1. Principal Component Analysis and fossil sampling bias

23 Paleontological data are intrinsic scarce (Strauss, Atanassov & Oliveira, 2003; Hammer, 2006),
24 leading to incomplete data sampling. This limitation impact several approaches on
25 paleontological studies, especially inter-specific variation analyses. Although there are some
26 approaches proposed to deal with missing entries in fossil datasets (e.g.: Norell & Wheeler,
27 2003; Strauss, Atanassov & Oliveira, 2003), sometimes the study relies on a statistic exploratory
28 evaluation of general structure in the data and Principal Component Analysis (PCA) is
29 commonly used to this purpose.

30 PCA is a multivariate and exploratory analysis. Its aim is to identify the variables that account
31 for the majority of the variance within a multivariate matrix, by means of linear combinations of
32 all variables, which are converted into components that are independent of each other. Hence,
33 PCA technique summarizes a large amount of the variance contained in the data
34 (Krzanowski,1979; Hammer, Harper & Ryan, 2001). It thus reduces a multidimensional space
35 into fewer components which retain the majority of the variance of the sample (Jolicoeur &
36 Mosimann, 1960; Peres-Neto, Jackson & Somers, 2003), becoming easier to make
37 interpretations on large data sets.

38 This approach has been largely applied to both extant and fossils vertebrates (e.g. Jolicoeur &
39 Mosimann, 1960; Claude et al., 2004; Depecker et al., 2005, 2006; Astua, 2009; Burnell, Collins

& Young, 2012; Costa, Moura & Feio, 2013; Bhullar et al., 2012; Fabre et al., 2014; Werneburg et al., 2014; Ferreira et al., 2015), as well as a matter of discussion on 70's and 80's years (e.g.Krzanowski, 1979, 1982; Corruccini, 1983; Somers, 1986, 1989; Sundberg, 1989) under the light of allometric interpretations.

1.2. Case-study

1.2.1. Skull variation

The skull is one of the most variable structures in vertebrates because it concentrates several sensory organs, the brain, and the beginning of the respiratory and digestory systems, including chewing muscles (Smith, 1993). Consequently, the skull is the body portion with more phenotypes used in vertebrate cladistic analysis (Rieppel, 1993), as seen in turtles, in which most cladistic analysis rely mainly on cranial characters (Gaffney, 1975; Gaffney et al., 1991; Meylan, 1996; Hirayama, 1994; Hirayama, 1998; Hirayama, Brinkman & Danilov, 2000; de la Fuente, 2003; Takahashi, Otsuka & Hirayama, 2003; Gaffney et al., 2006, 2011; Joyce, 2007; Joyce & Lyson, 2010; Lyson & Joyce, 2009, 2010; Sterli et al., 2010; Sterli & de la Fuente, 2011a, b; Gaffney & Krause, 2011; Anquetin, 2012; Rabi et al., 2013; Havlik, Joyce & Böhme, 2014; Romano et al., 2014; Brinkman et al., 2015; Ferreira et al., 2015; Sterli, de la Fuente & Krause, 2015). Despite that, most of skull materials found in paleontological record of turtles are unique and/or damaged due to the fossilization process bias, not allowing intraspecific studies or ontogenetic inferences on most fossil turtle species known.

1.2.2. *Bauruemys* taxonomy

Bauruemys elegans (Suárez, 1969) is a Late Cretaceous freshwater side-necked turtle found at the Pirapozinho site (Suárez, 2002). This species was originally described as *Podocnemis* in

three different communications by Suárez (1969a, b, c) and identification was based on the overall similarities of skull and shell to this living genus, a common practice at that time. Other South American Cretaceous side-necked turtles were initially identified as *Podocnemis* as well, such as the *nomina dubia "Roxochelys" harrisi* (Pacheco, 1913) and *"Bauruemys" brasiliensis* (Staeche, 1937) and the *incertae sedis "Podocnemis" argentinensis* (Cattoi & Freiberg, 1958) (see Romano et al., 2013 for a revision on Bauru Group species and Fig. 1). On a revision of *Bauruemys elegans*, Kischlat (1994) was the first to point out that all *Podocnemis* reported to the Cretaceous were doubtful and proposed a new genus to include *B. elegans* and, tentatively, *B. brasiliensis*. His approach was based on similarities of the plastron of both species. Kischlat (1994) and Kischlat et al. (1994) also pointed that *B. elegans* could belong to Podocnemididae, but they did not tested their hypothesis. Romano & Azevedo (2006) were the first to carry out a cladistic analysis to access the phylogenetic position of *Bauruemys*, placing it as a stem-Podocnemididae, i.e.: the sister group of all other Podocnemididae, which were confirmed by subsequent analysis including more podocnemidid species as terminals (França & Langer, 2006; Gaffney et al., 2011; Oliveira, 2011; Cadena, Bloch & Jaramillo, 2012).

1.2.3. Geological settings and taphonomic context of the Tartaruguito site

The Pirapozinho site, long ago known as "Tartaruguito" and formally assigned as such by Romano & Azevedo (2007) and Gaffney et al. (2011), is an Upper Cretaceous outcrop from the Presidente Prudente Formation, Bauru Basin (*sensu* Fernandes & Coimbra, 2000). It is located in Pirapozinho municipality, São Paulo State, Brazil (Fig. 1). The "Tartaruguito" name, which means "turtle in rock" (*tartaruga*, from Portuguese, turtle; *ito*, from Greek, rock), is due to the great amount of turtle specimens found at that place. It is comparable to other rich fossil turtle localities, such as (1) the recently found Middle Jurassic Qigu Formation of the Turpan Basin in

China (Wings et al., 2012; Rabi et al., 2013); (2) the Middle-Upper Paleocene Cerrejón Formation in Colombia (Jaramillo et al., 2007; Cadena et al., 2010; Cadena, Bloch & Jaramillo, 2012; Cadena et al., 2012); (3) and the Upper Miocene Urumaco Formation ('Capa de tortugas') in Venezuela (Aguilera, 2004; Sánchez-Villagra & Aguilera, 2006; Sánchez-Villagra & Winkler, 2006; Riff et al., 2010; de la Fuente, Sterli & Maniel, 2014). The two latter localities are near-shore marine coastal deposits with influence of freshwater rivers (Jaramillo et al, 2007; Gaffney et al., 2008), whereas the former and the Tartaruguito site correspond to rocks that had been deposited in a riverine system with seasonal droughts in which turtles gathered in retreating, ephemeral water pools and died when habitat dried up completely (Soares et al., 1980; Fulfaro and Perinotto, 1996; Fernandes & Coimbra, 2000; Henriques et al., 2002, 2005; Suárez, 2002; Bertini et al., 2006; Henriques, 2006; Wings et al., 2012). The Tartaruguito is also the type-locality of the Peirosauridae crocodile *Pepesuchus deiseae* Campos, Oliveira, Figueiredo, Riff, Azevedo, Carvalho & Kellner (2011).

The general lithology of the Tartaruguito site is composed of cyclic alternations of sandstones and mudstones deposited in a meandering fluvial system with crevasse splays (Fernandes & Coimbra, 2000; Henriques et al., 2005). Many articulated and complete fossils are found in these sequences, which indicate seasonal low energy floods (mudstones) followed by droughts (sandstones) in the region during Late Cretaceous (Henriques et al., 2002, 2005; Henriques, 2006). Because only medium- to big-sized fossil specimens are found at the locality, we believe that the Tartaruguito site was a foraging area for turtles (D. Henriques, pers. comm.). Thus, the fossil assemblage probably represents several episodes of floods and droughts. The flood periods might have allowed foraging areas expansion for turtles and crocodiles, while during the dry

seasons turtles gathered on the remnants of water pools and some died when pools dried up completely (Henriques et al., 2002, 2005; Henriques, 2006).

That being said, we consider that all turtle specimens found at the Tartaruguito site might correspond to subadults to adult ages, and that is reasonable to assume all *B. elegans* individuals collected in the Tartaruguito site might have belong to a single population (agreeing with Henriques et al., 2002, 2005; Henriques, 2006). Indeed, as pointed by Romano & Azevedo (2007), this single population would consist on different generations of turtles' corpses grouped in the same locality. One might consider that size differences might be due to sexual dimorphism (R. Hirayama and S. Thomson, pers. comm.), on which the females would be bigger and have more posteriorly extended carapaces than the males. However, sexual dimorphism on podocnemidid turtles can be accessed only on shell shape and our data is based mostly on isolated skulls (see Material and Methods). As consequence, although it is possible to have some sexual dimorphism size effect on our data, we do not considered it, given the lack of evidence to assume such outcome. Moreover, Romano & Azevedo (2007) were not able to reject the single population hypothesis using shell measurements (from both plastron and carapace) in a morphometric approach neither describe sexual dimorphism in the data, concluding that the differences were due to ontogeny variation among individuals from different generations. Therefore, we highlight that we are assuming the population definition of Futuyma (1993), as taken on by Romano & Azevedo (2007), that a population is a conjunct of semaforontes temporally connected, i.e., a sequence of individuals from different generations, and limited in a restrict space, in this case, the Tartaruguito site.

1.3. Objectives

Many fossil materials are housed in foreign collections and are not easily accessible by researchers. It can narrow and even preclude their studies. In addition, given the missing data problem inherent to fossil record, the way one lead with the missing entries in morphometric studies can affect the results and conclusions. Here we test a novel approach to take linear measurements for morphometric studies based on photographs of fossil materials. We also evaluate how different approaches desinged to deal with missing data can impact results of exploratory statistical procedures and data interpretation by comparing two different substitution algorithms of missing entries. These procedures are exemplified using a real paleontological data set and with a paleobiological inferences.

We carried out the same approach of Romano and Azevedo (2007) using cranial characters in order to explore the variation among individuals from different ages and generations – then, assuming Henning's (1966) semaphoront concept to the specimens of our sample. Also, we described the differences in skull morphology along the ontogeny of *B. elegans* and the probably consequences of such variation to the diet preferences changes along the growth.

2. Material and Methods

2.1. Sample and characters

Twenty one skulls of *Bauruemys elegans* were examined in this study: AMNH-7888, LPRP0200, LPRP0369, LPRP0370, MCT 1492-R (holotype), MCT 1753-R (paratype), MCZ 4123, MN 4322-V, MN 4324-V, MN 6750-V, MN 6783-V, MN 6786-V, MN 6787-V, MN 6808-V, MN 7017-V, MN 7071-V, MZSP-PV29, MZSP-PV30, MZSP-PV32, MZSP-PV34, and MZSP-PV35. We established 39 landmarks (Fig. 2) that decompose the overall shape of the skull in order to take measurements between two landmarks. Moreover, since most of the specimens

151 have deformation and breakage, we could not perform a geometric morphometric analysis using
152 the landmarks because the taphonomical bias would incorporate error to the analysis of form and
153 shape. Thus, we used the landmarks to set up 29 traditional morphometric characters that
154 correspond to a linear measurement between two landmarks (all characters are described on table
155 1). Also, the use of landmarks to set up the measurements is useful to maintain the same
156 anatomic references for all characters in each specimen, since the landmarks enable a better
157 description of morphological variation and establishment of quantitative characters, as
158 exemplified by Romano & Azevedo (2007). All measurements were taken by TFM in the same
159 side of the skull (right side) unless the characters could not be measurable due to deformation or
160 breakage. We used ImageJ version 1.47 (Rasband, 1997) to take the measurements after
161 comparing its accuracy with the caliper (Mariani & Romano, 2014). This procedure was
162 necessary because PSRR obtained photos of skulls housed in foreign collections and did not
163 perform measurements by caliper. The error test between measurements taken using caliper and
164 ImageJ are described bellow. We followed the bone nomenclature of Parsons & Williams (1961)
165 and extended by Gaffney (1972, 1979) (see all abbreviations after Conclusion topic).

166 **2.2. Statistical Analysis**

167 Before carrying out the statistical analysis, we compared the same characters data set (Data S1)
168 of the same sample by using two different approaches (= treatments): measurements taken using
169 caliper and measurements taken using photographs via ImageJ. This comparison was necessary
170 in order to evaluate whether or not the two measurements methods are significantly different.
171 Then, we performed an One-way Analysis of Variance (ANOVA) comparing the 29
172 measurements in 12 specimens (LPRP0200, LPRP0369, LPRP0370, MN4322-V MN4324-V,
173 MN6750-V, MN6783-V, MN6786-V, MN6787-V, MN6808-V, MN7017-V, and MN7071-V).

Two groups of variables were established: measurements taken directly from specimens using caliper (preliminary data set 1) and the same characters taken from photographs of the same specimens using ImageJ (preliminary data set 2). All characters taken using photographs/ImageJ that did not show significant differences to their correspondents taken by caliper were used on the subsequent statistical analyses of form and shape differences among the sample of *Bauruemys elegans*. By doing that, the sample was increased without including error and incomparable characters (i.e.: by using different measurement techniques).

Three analyses using the complete sample were carried out: (1) a descriptive statistics (mean, standard deviation, median, variance, maximum and minimum values) of all characters (Data S2), (2) an allometric analysis of length and width characters correlating them to total length and width measurements (Data S3), and (3) a multivariate non-parametric exploratory statistics via Principal Component Analysis (PCA). The later was divided into two different PCA: (3.1) using 27 characters from the raw data matrix (total lenght and width characters were excluded in this analysis; Data S4), and (3.2) using 27 charactes that represent proportions of each length and width characters in relation with total length and width characters, respectively (Data S5). All statistical analysis were performed using the software PAST version 3.05 (Hammer et al., 2001).

In the first PCA approach (3.1) we excluded total length and width characters because of its high influence in the PCA result, since higher values compose the majority of the summarized variance in PC's (Mingoti, 2013), and because of the redundance between these measurements and the others. We also assessed differences by applying two different substitution algorithms for missing data in PAST, using the default "mean value imputation" option (i.e. missing data are replaced by the column average), and the alternative "iterative imputation" option, which computes a regression upon an initial PCA until it converges to missing data estimations,

197 replacing missing data by such estimations (Ilin & Raiko, 2010). The latter is recommended and,
198 after comparing both results, we selected it (see supplemental material 3 to visualize PCA results
199 computed using PAST's default option approach). The second PCA (3.2) was conducted to
200 remove effect of size and perform an exploratory analysis of the shape alone. Six specimens
201 were removed from this second analysis because were broken and the total length or width
202 measures were not measurable.

203 The first analysis was made in order to quantify and describe the variation of the characters set in
204 *Bauruemys elegans* skull, using the assumption of the sample be representative of a single
205 population. The second analysis allowed us to make inferences about osteological shape change
206 related to size change, i.e., related to growth, by assuming that bigger specimens are older than
207 smaller ones. This approach is, therefore, a study of allometry (Huxley & Teissier, 1936; Huxley,
208 1950; Gould, 1966; Gould, 1979; Somers, 1989; Futuyma, 1993) and the assumption of
209 correlation between size and aging is based on continuous growth to be common on extant turtles
210 (Klinger & Musick, 1995; Shine & Iverson, 1995; Congdon et al., 2003). The PCA analyses
211 were carried out in order to evaluate if there are some structuring in the data through the
212 reduction of the variation into orthogonal axes which retains most of the variance. Since the use
213 of a parametric statistic was infeasible due to the nature of the sample (i.e.: a small matrix that do
214 not show homoscedasticity and normality in data set), the PCAs were used to search for a
215 structure of the data that matches to that illustrated by Romano & Azevedo (2007) using
216 postcranial characters. If the pattern observed is similar to previous morphometric and
217 taphonomic inferences, then it is interpreted as not enough existing evidence to assume the
218 sample represents different populations of *Bauruemys elegans*. In other words, since a parametric

test is not feasible with statistical confidence, the lack of structure in the PCAs projections were herein interpreted as a fail to the attempt of falsifying the single population hypothesis.

3. Results

3.1. Does caliper differ from images?

The results of ANOVA are summarized in table 1. We found most of measurements do not differ statistically ($p>0.05$) between the two treatments (caliper and ImageJ). However, one measurement, length of maxilla (LMX), had statistical difference ($p=0.017$) between the treatments (see discussion). Because of this result, we increased our sample from 12 to 21 specimens.

3.2. Descriptive Analysis

The results of the descriptive statistics are summarized in table 2. As expected values of total length and width (TLS and WLS) were the most variable in comparison with others, because the variation scale in these characters is greater than in others. Characters of the bones forming the upper temporal fossa (i.e. PA, QJ, SQ, QU and OP) had great variation, being parietal the most variable in lenght (SD=6.45) and the smallest in width (SD=2.94), whereas quadratojugal obtained the smallest variation in lenght (SD=2.38) and the greatest in width (SD=4.03). Among the characters of the bones forming the lower temporal fossa (i.e. JU, MX, PO, PT and PAL), the variation in lenght was in general greater than in width. Postorbital and maxilla had almost the same variation in lenght (SD=4.12 and SD=4.11, respectively); WPO had the smallest variation within the group of bones forming the lower temporal fossa (SD=1.83); and the strecth of the maxilla had the greatest variation (SD=7.63) of all characters measured. Characters of the other bones had smaller values than the aforementioned bones, with the exception of WPO which was

smaller than LFR (SD=2.08), LVO (SD=1.95), LBO (SD=2.12),WFR (SD=1.88) and WBS (SD=2.19).

3.3. Allometric Analysis

Among all comprised measurements, three were truly negatively allometric (LPF, WJU and WQJ); five were positively allometric (LPAL, LPT, LPO, WPF and WPO); and the others were negatively allometric. It is also worth to note that two were virtually isometric [WPF (a=1,0074) and WOP (a=0.98159)]. All regressions are shown on figures 3, 4 and 5.

3.4. Principal Component Analysis (PCA)

3.4.1. Raw data

3.4.1.1. Replacing missing data with mean values

By using the "mean value imputation" approach, a total of 70.32% of the variance was comprised by the first three principal components (PC1=42.15%; PC2=16.82%; PC3=11.35%), so that the others were less significant for the analysis and are not presented. We interpreted that PC1 variation is due to size change-over because an approach using all characters have shown a similar result. PC2 and PC3 seems to represent shape differences between individuals. In all PC individual projections (Fig. 6A and 6B) most of specimens were included inside the 95% ellipse. Two exceptions are MCZ4123 and MN7071-V, which have not been included in the ellipse when PC1 vs. PC2 were considered (Fig. 6A); also the former was outside the ellipse in PC2 vs. PC3 scatter plot (Fig. 6B), indicating shape differences of these specimens. However, both specimens have suffered different degrees of crushing due to taphonomic bias and that is likely the reason for this result.

In PC1' loadings (L; Table 3), only two characters were negatively related (LPF and WJU); SMX, LPA and LPO loadings were the highest related (L=0.69; L=0.27; L=0.36, respectively); and the rest of characters obtained intermediate values [e.g. LPT (L=0.17), LMX (L=0.18), WOP (L=0.21)]. PC2 has shown a high relation with character LPA (L=0.77), showing possible changes in shape in this region, and a negative loading for SMX (L= -0.38), whereas the others had no significant scores. The last considered principal component (=PC3), showed high correlations with bones in both lateral and posterior emarginations of the skull [LMX (L=0.68), WMX (L=0.25), LJU (L=0.30), WQJ (L=0.29) and LQU (L=0.32)] and, as the results in PC2, allows inferences in shape changes of these regions.

3.4.1.2. Replacing missing data with regression estimation

The alternative missing data approach (i.e. "iterative imputation"; Fig. 6C) generated two principal components which comprised 88.96% of the total variance (PC1=53.01%; PC2=35.95%). In contrast with the previous approach, PC1 was interpreted as shape, whereas PC2 as size. In addition, all specimens were included inside the 95% ellipse in PC1xPC2 scatter plot. The specimen MN7017-V, interestingly, was excluded from the ellipse when considering PC2 vs. PC3, but the percentage of variance represented by PC3 is too low (PC3=3.28%) to assume any difference from the others individuals. We agree with Ilin & Raiko (2010) and prefer to choose the iterative imputation approach for dealing with missing entries (see discussion on session 4.2. "The single population hypothesis"). Then, discussions concerning the form variation in our data are related to PCA analysis using iterative imputation.

In PC1 loadings (Table 3), LPA, WPA and LSQ were the highest positively related characters (L=0.89; L=0.22; L=0.16, respectively), whereas LMX, LJU, LQJ, WQJ and LQU were the

highest negatively related characters (L= -0.18; L= -0.14; L= -0.16; L= -0.11; L= -0.11; L= -0.13, respectively). Only two characters were negative for PC2 (LPF and WJU), whereas the rest of the coefficients were positive. Among them, SMX was the highest (L=0.59); WPAL, WBS, LBO, LJU, LQU, LPO and WOP obtained intermediate scores (L=0.23; L=0.19; L=0.20; L=0.19; L=0.21; L=0.29; L=0.30, respectively); the others were less related [e.g. LPA (L=0.04), LPT (L=0.13) and WPO (L=0.10)]. In general, the values indicate that in *B. elegans* most changes occur in bones of both lateral and temporal emargination.

3.4.2. Shape characters (proportions)

3.4.2.1. Replacing missing data with mean values

When applying "mean value imputation", 53.99% of the variance were comprised by the first two principal components (PC1=35.29%; PC2=18.70%), both corresponding to shape, as all units of measurements were removed through the ratio of characters before carrying out the analysis. All specimens were comprised into the 95% ellipse (Fig. 7A).

The first PC was positively related to the loadings values of LPA/TLS (L=0.28), LMX/TLS (L=0.38), LQU/TLS (L=0.27), WPA/TWS (L=0.23), SMX/TWS (L=0.38), WMX/WTS (L=0.35), WQJ/TWS (L=0.48); the most negative values were LPO/TLS (L= -0.16) and WOP/TWS (L= -0.13). The second PC was positively related to LPA/TLS (L=0.66), WPA/TWS (L=0.32)WOP/TWS (L=0.27), and negatively to LMX/TLS (L= -0.50) (see Table 4 for all loading values). It is interesting to note that most of highly-related proportions were in reference to bones associated either with feeding *apparatus* (squamosal, parietal, quadratojugal and jugal) or catching food and trituration surface (maxilla).

3.4.2.2. Replacing missing data with regression estimation

The "iterative imputation" substitution model of missing data resulted in 77.35% of the variance comprised by two principal components (PC1=45.49%; PC2=31.86), both representing shape. All specimens were included in the ellipse (Fig. 7B), thus shape differences do not indicate possible different populations or species.

PC1 was highly related to LMX/TLS (L=0.48), LJU/TLS (L=0.16), LQJ/TLS (L=0.21), LQU/TLS (L=0.28), LSQ/TLS (L=0.20), SMX/TWS (L=0.33), WMX/TWS (L=0.30), WJU/TWS (L=0.26) and WQJ/TWS (L=0.41), which represent the highest values as well as bones constituting both lateral and posterior emargination. Conversely, PC2 was mostly represented by LPA/TLS (L=0.67), LSQ/TLS (L=0.34) and WPA/TWS (L=0.33) (see Table 4). These loadings represent shape changes in regions of the skull that are associated with muscles' attachment as well as trituration surfaces (see below).

4. Discussion

4.1. Replacing the caliper by ImageJ

Almost all measurements did not differ between the two treatments, and only one measurement (= length of maxilla, LMX) had the opposite result. This indicates that ImageJ is an useful tool in replacing the use of caliper (see table 1). Although we found no statistical differences for many of the measurements, we had difficulties in taking some of them and we must discuss it herein. First, because of taphonomical processess, many cracks appears in the photos and can be confused with sutures between bones. Thus, a previous anatomical knowledge of the material is very helpful. Second, we had difficulties in identifying some landmarks due to overlapping structures or badly focused region. The first problem cannot be solved for one cannot break a piece of the material, and taking pictures from a different angle will lead to a measure different

from the reality. The second is easily solved by a good accuracy in focusing the image, and by taking pictures in different focus.

Another problem is related to the result we found for LMX. Such a result is due to the optical processes that occurs in the camera. Photos are two dimensioned images and, for that reason, deeper points are not captured in their real positions because they are farther from the camera. Because of the anatomically curved shape of the maxilla, the rostralmost landmark (LM 24) established to take this measurement is deeper in relation to the caudalmost landmark (LM 11), which is also the plane the picture was taken. As a consequence, the straight line between landmarks 11 and 24 (used to take LMX) is smaller than the real line and this measurement is underestimated. This is also the case for steep structures. Therefore, one should be careful when establishing the landmarks and measurements in specimens with many curvatures and steep estructures.

Despite this, the study *in situ* of the material is preferable, although pictures are an economic alternative in cases one are not able to handle the material. We must aware that one have to choose one of the two treatments to construct a morphometric matrix, otherwise it will be composed of values obtained by two diffent methods.

4.2. The single population hypothesis

In this section, we discuss our results by tackling in two fronts, one underlied on the taphonomy of the Tartaruguito locality, and another on the taxonomy of the valid fossil turtle species of the Bauru Group. The former will be taken briefly, since it is well stablished on the literature, the latter is more carefully considered because it is still a matter of debate among paleontologists.

4.2.1. The depositional context at the "Tartaruguito" site

The depositional environment at the Pirapozinho site is well-known from previous studies, which point out to seasonal floods in which turtles might have gathered in water bodies for foraging, followed by droughts that caused their death (Soares et al., 1980; Fulfaro and Perinotto, 1996; Fernandes & Coimbra, 2000; Henriques et al., 2002, 2005; Suárez, 2002; Bertini et al., 2006; Henriques, 2006). This is, consequently, a case of several seasonal non-selective death events, with individuals representing semaforonts connected temporally (between generations), thus comprising a single population (agreeing with Futuyma, 1993 population definition and used by Romano & Azevedo, 2007). We failed to disprove the null hypothesis that all individuals belong to a same population of *Bauruemys elegans*, agreeing with Romano & Azevedo (2007) conclusion using post-cranium data.

4.2.2. Taxonomic considerations between B. elegans *and other species of Bauru Basin*

Many skulls sampled have taphonomic effects, such as cracks and crushes. For instance, MN7071-V is notably the biggest specimen of the sample and is represented in the uppermost positive side of the size-related PC2 axis (Fig. 6C). Although it is indeed a big specimen, it was clearly a taphonomic effect (crushing) that caused its bigger size. On the other hand, Bertini et al. (2006) indicated that turtle bodies have suffered little transportation or crushing in Tartaruguito site. We agree with this taphonomical interpretation of the site but, although most specimens do not show huge breaks, these distortions might mask morphometric interpretation (the case of MN7071-V).

Another aspect is the presence of polymorphism in *B. elegans*. Romano (2008) presented an unusual carapace for the specimen MN7017-V, as having a seventh neural bone, differing from the diagnostic number of six neurals for this species, and with the diagnostic four-squared second

neural bone not contacting first costals (Suarez, 1969; Kischlat, 1994; Gaffney et al., 2011). The morphometric analysis performed by Romano (2008) did not revealed significant statistical differences between MN 7017-V and other *B. elegans* specimens. We have also included the MN7017-V skull in our analysis, and there was no variation to state anything apart from Romano's (2008) conclusion that it is probably a polymorphic *B. elegans* specimen (Fig. 6C). Still, we reevaluated this skull and found the diagnosis characters for *B. elegans*. Therefore, all skulls included in our study belong to the same species (i.e. *B. elegans*).

Among the five valid fossil turtle species found throughout the Bauru Basin, only two have been collected at the Pirapozinho site so far (Romano et al., 2013). The first is *B. elegans*, which is recognized by both skull and shell materials; the second is *Roxochelys wanderleyi* Price, 1953, based only on shell material (de Broin, 1991; Oliveira & Romano, 2007; Romano & Azevedo, 2007; Gaffney et al., 2011; Romano et al., 2013). So far, none *R. wanderleyi* with skull-shell associated body parts were collected. It is possible that the chelonian fauna of the Bauru Basin might be overdimensioned (Romano et al., 2009, 2013). Then, the two new skull-only species from the Caiera Quarry recently described, *Peiropemys mezzalirai* and *Pricemys caiera* (Gaffney et al., 2011), might be a representative skull material of *R. wanderleyi*. However, we cannot claim that until a skull-shell *R. wanderleyi* specimen be found.

4.3. Ontogenetic changes in *B. elegans* skull

Once we have assessed that all specimens belong to the same species and population, we are able to discuss the skull variation in the sample assuming as due to inter-populational variety. For the sake of organization, we divided the discussion into two parts, based on the anatomical regions of the turtle skull: upper temporal fossa and lower temporal fossa, following Schumacher (1973),

Gaffney (1979) and Gaffney et al. (2006). We have chosen this organization because the bones we found most association with the principal components in the two PCA analyses compose these two regions and are generally involved in aspects of the feeding mechanisms of turtles, either as muscles attachments or forming triturating surfaces.

4.3.1. Bones of the upper temporal fossa and skull roofing

The temporal emargination of podocnemidid turtles is formed by the dorsal, horizontal plate of the parietal, the quadratojugal and the squamosal, with no contribution of the postorbital (Gaffney, 1979; Gaffney et al., 2011). This region (and bones) is associated to the origin of the adductor muscle fibers (m. adductor complex; Fig. 9A and 9B) (Schumacher, 1973; Werneburg, 2011; Werneburg, 2012; Jones et al., 2012; Werneburg, 2013), which run through *cartilago transiliens* of the *processus trochlearis pterygoidei* of the pterygoid and insert at the coronoid process of the lower jaw (Schumacher, 1973; Gaffney, 1975; Gaffney, 1979; Lemell et al., 2000; Werneburg, 2011). These muscles promote the closure of the mouth, thus it is reasonable to associate the attachment surface to bite force and the latter to the prey hardness. Yet, on the ventral flange of the squamosal origins the muscle *depressor mandibulae* (Schumacher, 1973; Gaffney et al., 2006; Werneburg, 2011; Fig. 9B), which cause the abduction (=opening) of the mandible.

The variation in this area of the skull in turtles was a matter of some studies (e.g. Dalrymple, 1977; Claude et al., 2004; Pfaller et al., 2011), which indicated allometric ontogenetic growing patterns of the bones in these regions. Such authors were able to identify a high correlation with the increasing of muscle mass and shift in feeding features (Dalrymple, 1977; Pfaller et al., 2010; Pfaller et al., 2011). Moreover, there are changes in skull shape associated to the aquatic

environment and foraging strategies, as suggested for emydids and testudinoids turtles by Claude et al. (2004). Although these studies focused on hide-necked turtles, the same morphoecological patterns can be applied to side-necked turtles, since there are habitat occupation similarities between side-necked and hide-necked turtles with implications to the skull morphology due to morphofunctional constraints (Schumacher, 1973; Lemell et al., 2000), besides the adaptive selection regarding fresh water feeding strategies (see Lauder & Prendergast, 1992, Aerts et al., 2001 and Van Damme & Aerts, 2001 for feeding strategies in freshwater turtles).

The high variance and positive allometric growth of the parietal (LPA: a=0.38; WPA: a=0.32), quadratojugal (LQJ: a=0.16; WQJ: a= -0.06) and squamosal (LSQ: a=0.30) lead to an increasing in temporal emargination and, consequently, a greater area for attachment of the external adductor muscle. The consequence of this would be the generation of large forces and high velocities during the fast closing phase of an aquatic feeder, as seen in *Pelusios castaneus* (Lemell et al., 2000), and even a more powerful bite for crushing harder prey, as seen in *Sternotherus minor* (Pfaller et al., 2011). In addition, the lenghthen of the squamosal would allow a greater insertion area of the m. *depressor mandibulae* and muscles of the hyobranchial apparatus (e.g. m. constrictor colli) (Schumacher, 1973; Gaffney, 1979; Claude et al., 2004; Gaffney et al., 2011; Werneburg, 2011). The m. *depressor mandibulae* is useful for an increased gape opening speed and the hyobranchial apparatus musculature is involved in backwards water flow generation by the lowering of the hyoid apparatus, two characteristics well reported for other pleurodire turtles (e.g.Van Damme & Aerts, 1997; Aerts et al., 2001; Lemell et al., 2000; Lemell et al., 2002). Moreover, Claude et al. (2004) demonstrated that aquatic turtles with suction feeding mode possess longer skulls than terrestrial turtles, being squamosal the most

proeminent bone involved in this elongation and functionally related to the style of prey capture (= suction) as a support for mandible and hyoid muscles.

Also, Gaffney et al. (2011), in a comparison with other podocnemidid turtles, indicated *B. elegans* as having a "skull relatively wide and flat" (p. 12), which could be observed by the increasing of some bones, specially the postorbital (Figs. 3G and 4H), parietal (Fig. 3A and 3J), quadratojugal (Figs.3I and 4F) and jugal (Figs. 3C and 5B). Comparing the postorbital allometry (better discussed below) with those of the bones in contact with it in the skull roof (frontal, parietal, jugal and quadratojugal; Gaffney et al., 2011), we observe an influence of the positive growth of the former into the others, leading to flattening and widening of the skull.

In a study assessing the bite performance in turtles, Herrel et al. (2002) suggested that a higher skull is efficient in promoting stronger bite forces, specially in species which feed on hard prey, but they also pointed out that additions in bite forces may be achieved by "getting longer and larger" skull with no increasing in skull height. Thus, in addition to provide gains in muscle attachment area, by the growing of parietal, quadratojugal and squamosal, leading to a longer skull, a stronger bite and possibly a change in diet along the ontogeny. Also, the allometric growths of most of skull bones, particularly the positive allometry of the postorbital, indicate a more roofed skull in *B. elegans* adults. Given the allometric patterns aforementioned, *B. elegans* might have had a wide and flat but a long skull, which would have compensate the loss of muscle volume and attachment area caused by widening and flattening the skull (Herrel et al., 2002). Correlations between a more emarginated skull and increases in the volume of the adductor muscle were also explored in a cranial evolutionary framework of stem-turtles by Sterli and de la Fuente (2010).

460 At last, Gaffney et al. (2006, 2011) scored a character based upon the contact between
461 quadratojugal and parietal bones (char. 13 of Gaffney et al., 2006; char. 5 of Gaffney et al.,
462 2011). They also state that this contact is present in *Hamadachelys* + Podocnemididae clade,
463 with a large quadratojugal (state 1), in contrast to most of other Pelomedusoides (state 0: contact
464 absent in Pelomedusidae, Araripemydidae and many bothremydids (e.g. Kurmademydini,
465 Cearachelyini and Bothremydini); state 2: contact present with small quadratojugal in some
466 Taphrosphyini, Bothremydidae). Indeed *B. elegans* possess a large quadratojugal, which means
467 that the reduction of postorbital evolved after *Bauruemys* node of divergence. However, we
468 found a greater increasing (positive allometry) of the two measurements of the postorbital and
469 this might have influenced the growth of parietal and quadratojugal, as well as the jugal (see
470 below), so that the state 1 seen in *B. elegans* is possibly a consequence of allometric changes.
471 This is easily seen if the truly negative allometry of the width of the quadratojugal (WQJ: a=-
472 0.06) and the slight increasing in the length of this bone (LQJ: a=0.16) are compared with the
473 postorbital measurements. It also could have influenced the growth of the parietal, but in a less
474 degree, as seen in the allometries of this bone (LPA: a=0.38; WPA: a=0.32).

475 When comparing the stem-Podocnemidinura species (i.e. *Brasilemys*, *Hamadachelys*) and stem-
476 Podocnemididae (e.g. *Bauruemys*, *Peiropemys*, *Pricemys* and *Lapparentemys*), with the
477 Podocnemidodda (i.e. Podocnemidand + Erymnochelydand) (Gaffney et al., 2011; Fig. 8), it is
478 clear that an increasing in the parietal-quadratojugal contact has occurred along the
479 podocnemidid lineage, and consequently led to a more roofed skull and to a less emarginated
480 skull. We suggest that in *B. elegans* the small contact is due to the positive growth of the
481 postorbital resulting in a more emarginated skull than other podocnemidids, as described by
482 Gaffney et al. (2011). Yet, within Podocnemidand this bone suffered the opposite effect (i.e.

small growth), showing variations in size and even being absent in some species (e.g. *Podocnemis sextuberculata*; Ruckes, 1937; Gaffney, 1979; Gaffney et al., 2011), though the emargination is still great. On the other hand, in Erymnochelydand the postorbitals are large but the quadratojugal and parietal are large as well, leading to a greater contact between these bones and a well-roofed but less emarginated skull, being a reversion in *Bairdemys venezuelensis* and *B. sanchezi* within Erymnochelydand (Gaffney et al., 2011). Therefore, the increasing or decreasing in the temporal emargination within Podocnemididae could be due to variation of allometric patterns in bones that form the skull roof, particularly the postorbital, quadratojugal and parietal, among different lineages.

4.3.2. Bones of the lower temporal fossa

The lower adductor chamber in Pelomedusoides is formed externally and laterally by the jugal and quadratojugal, with the addition of the maxilla in some cases (e.g.: *Podocnemis* spp. and *Bairdemys sanchezi*). The well developed cheek emargination, found in most but not all podocnemidid turtles (the exceptions are many species of Erymnochelydand, but not *Bairdemys* spp., *Cordichelys antiqua* and *Latentemys plowdeni*), is also part of the adductor chamber (Gaffney, 1979; Gaffney et al., 2006; Gaffney et al., 2011). Internally and medially, the postorbital, the jugal and the pterygoid compose the *septum orbitotemporale*, partially separating the *fossa orbitalis* from the *fossa temporalis*; along with the palatine, they aid to suport the *processus trochlearis pterygoidei* of the pterygoid (Gaffney, 1975; Gaffney 1979; Gaffney et al., 2006). There is a passage medially to the process of the pterygoid and the *septum orbitotemporale*, running from the *fossa orbitalis* to the *fossa temporalis*, the *sulcus palatinopterygoideus*. The palatine and pterygoid form the floor of its passage, while the parietal, postorbital and frontal limit its upper portion. In this region, the external adductor fibers run

506 through the *processus trochlaris pterygoidei*, and the internal adductor muscle (i.e. pterygoideus
507 muscle and pars pseudotemporalis; Fig. 9B) mostly origins throughout the pterygoid and parietal
508 bones (Schumacher, 1973; Lemell et al., 2000; Lemell et al., 2002; Werneburg, 2011). The
509 internal adductor fibers are involved in the jaw-closure system by generating counter forces
510 (protraction) to the external adductor (retraction) (Schumacher, 1973; Lemell et al., 2000; Lemell
511 et al., 2002; Fig. 9C and 9D).

512 Variation of the upper temporal fossa has been studied in different turtles, such as various
513 trionychids (Dalrymple, 1977) and *Chelydra serpentina* (Herrel et al., 2002). However, few
514 studies report on the variation of the lower adductor chamber, although both the temporal fossa
515 as well as the latter are anatomically and functionally coupled (Schumacher, 1973). Dalrymple
516 (1977) identified a positve allometry in the width of the "temporal passageway" in trionychids.
517 This area is related to the cryptodire pulley system (i.e. a *processus trochlearis* formed by the
518 quadrate and opisthotic) and is analogous to the pleurodire pterygoid process, and thus can be
519 comparable functionally (Gaffney, 1979). Herrel et al. (2002) concluded that the increase of the
520 bite force in turtles is due to either the increased height of the skull, leading to a more open angle
521 of the *processus trochlearis* in relation to skull longitudinal axis, or to enlargement (in width and
522 lenght) of the skull, because it allows more area for muscle attachment and volume. We observed
523 the same pattern of growth change in *B. elegans*, as evidenced by the positive allometry of the
524 bones parietal, postorbital, palatine and pterygoid. Other features were observed by Dalrymple
525 (1977) in trionychids (e.g. height and width of the supraoccipital crest, lengthen of the squamosal
526 crest and a development of a horizontal crest in the parietal) and were correlated to changes in
527 skull shape with a shift in feeding habits, from softer to harder preys as individuals age. Again, it

seems to be the case of *B. elegans*, as evidenced by the positive allometry of the bones squamosal and parietal.

The bones that mainly compose the skull rostrolaterally and the lateral emargination revealed a correlated allometric shape shift. Even so jugal and maxilla showed small allometric variation (Figs. 4B, 4C, 6A, and 6B). The reduction of the jugal (WJU: a= -0.23) and quadratojugal (WQJ: a= -0.06) along with the small growth of maxilla (WMX: a=0.19) demonstrate a decrease in height at the anterior portion of the skull. Because of the contact between jugal and quadratojugal with postorbital (and its increasing; see previous topic), we suggest that the latter would possibly has affected the growth of the formers. Moreover, the strong development of the postorbital would ultimately affect the width of the maxilla, which in turn would also affect the jugal. In contrast, the lenghthen of this bone would be less affected (LMX: a=0.39). In addition, there is a considerable increment in the stretch of maxilla (SMX: a=0.70) (Fig. 3H) leading to a broader rostrum. Yet, this could allow a greater area for crushing (Kischlat, 1994) during ontogenetic growth. All these allometric changes indicate that *B. elegans* owns a more flattened and wider skull (Gaffney et al., 2011), which could have allowed greater bite forces generation (Herrel et al., 2002).

There are other morphological implications in which the lower adductor chamber bones are involved and that worth discussion. As previously pointed, three bones compose the *septum orbitotemporale*: pterygoid, jugal and postorbital (Gaffney, 1979; Gaffney et al., 2006). Together with palatine, these three bones provide support for the *processus trochlearis pterygoidei*, where runs the tendon that connect the external adductor complex into the lower jaw (Schumacher, 1973; Gaffney, 1975; Gaffney 1979; Lemell et al., 2000; Gaffney et al., 2006; Werneburg, 2011). Nearby the process, many muscle fibers origin or cross towards their insertions points

(Schumacher, 1973; Werneburg, 2011). The temporal emargination at the upper adductor chamber becomes more emarginted during growth. As a consequence, the attachment area for external adductor muscles increase during aging, potentially generating stronger bite forces. The consequence of this temporal emargination indentation is that the trochlear process would must be more robust to support higher forces. We interpret that the positive allometries of pterygoid (LPT a=1.37), postorbital (LPO a=1.25 and WPO a=1.36), and palatine (LPAL a=1.11) could be a response to this robustness of the trochlerar process during growth. In other words, they would act together by giving more resistance to the area in which the high forces created by the external adductors are applied. Gaffney (1979) suggested this robustness occurs because muscle volume increase and, consequently, higher bite forces, so these three bones would reinforce the *septum orbitotemporale* to support and not to break when muscles are contracted. In addition to such reinforcement, the growth of palatine could be associated to a larger area for crushing preys such as mollusks and crustaceans, as pointed out by Kischlat (1994).

The internal and posterior adductor muscles (Fig. 9B), which origin at the quadrate, prootic, pterygoid, palatine, postorbital and the descending process of the parietal (Schumacher, 1973; Werneburg, 2011), are important during the jaw-closure phase. The importance of these muscles has been debated for early tetrapods with flat skull and aquatic lifestyle (e.g. Temnospondyli and Lepospondyli; Frazzetta, 1968), in which the internal muscle might have assumed the main function of closing the jaw (Werneburg, 2012). This also occurs in turtles with flat skulls and with poorly developed crista supraoccipitalis (e.g. Chelidae; Werneburg, 2011; Werneburg, 2012). However, *B. elegans* does not have a skull as flat as chelids, but has a long supraoccipital bone as well as a greater emargination (Gaffney et al., 2011), indicating more area and volume to external adductor muscles (Dalrymple, 1977; Sterli & de la Fuente, 2010). The mechanical

574 effects of adductor muscles upon the lower jaw during food capture has been demostrated in
575 some turtles (Schumacher, 1973; Lemell et al., 2000; Lemell et al., 2002; Pfaller et al., 2011).
576 These studies agree that besides acting to close the mouth, internal adductors execute counter
577 protraction forces to the external adductors retraction forces, while posterior adductors produce
578 medial forces (Fig. 10C and 10D). The contraction of all these muscles together avoid
579 displacements of the mandible and reduce stresses at the articulation (Schumacher, 1973; Lemell
580 et al., 2000; Lemell et al., 2002). The positive allometries of the bones of the lower adductor
581 chamber of *B. elegans*, therefore, may reflect greater resistance for a more robust musculature of
582 internal and posterior adductors in response to higher forces created by external adductors.
583 Besides, these muscles also play the main role in feeding, as proposed for aquatic feeders
584 (Frazzetta, 1968; Werneburg, 2012), in addition to a larger area between the two tips of the
585 maxilla (i.e. SMX a=0.70) and a flattened skull.

586 **4.4. Feeding changes along ontogeny in *B. elegans***

587 Changes in skull shape may be due to habitat differences in which on-land turtles (e.g.
588 testudinids) possess higher and shorter skulls while aquatic turltes (e.g. emydids) own flatter and
589 longer skulls (Claude et al., 2004). The changes in skull shape of turtles along ontogeny have
590 been assessed in living species (Dalrymple, 1977; Pfaller et al., 2011). Generally, it is supported
591 that a diet shift occurs from small soft prey to bigger harder ones, in association with higher,
592 larger and more robust skulls. These, in turn, are more suitable for crushing clams and/or to
593 capture fishes by having a greater gape. The overall aquatic morphology comprises adaptations
594 to suction feeding, which was also discussed by Herrel et al. (2002), and could be the case of *B.*
595 *elegans*. Firstly because taphonomic studies at Pirapozinho site suggested a riverine ephemerous
596 system (Soares et al., 1980; Fulfaro and Perinotto, 1996; Fernandes & Coimbra, 2000; Henriques

et al., 2002, 2005; Suárez, 2002; Bertini et al., 2006; Henriques, 2006) and fossils with little transportion (Bertini et al., 2006), thus *B. elegans* must have been a semi-aquatic turtle, similar to the extant freshwater turtles. Secondly, the general pattern observed revealed form and shape changes in both temporal and lateral emargination (upper and lower adductor chamber, respectively): as a whole, *B. elegans* skull seems to become more emarginated, flattened and longer as it grows in, according to the skull shape for aquatic turtles found by Claude et al. (2004), and indicating greater area and volume for muscles attachment. In addition, the deeper temporal emargination of *B. elegans* indicates a greater increse in muscle volume (Kischlat, 1994), thus leading to a stronger bite force (Sterli & de la Fuente, 2010). This leads us to interpret such changes as related to shift in diet as individuals grow instead of shift in habitat.

Malvasio et al. (2003) described diet changes in *Podocnemis expansa*, *P. unifilis* and *P. sexturberculata* due to aging, concluding that the latter is a carnivore species whereas the two former are omnivorous. Whereas *P. expansa* changes its diet towards a more herbivorous, *P. unifilis* remains more balanced with similar ingestion of vegetables and meat (Malvasio et al., 2003). Although more work is necessary to elucidate this issue in *Podocnemis* spp, the allometric variation found in *B. elegans* suggests that it might has been accompanied by changes in diet along ontogeny.

Although we cannot have certainty of which food items the individuals of *B. elegans* might have eaten along their lives, we have evidences that point to a shift in diet along ontogeny. Besides the allometric patterns and loadings values indicating skull changes associated to adductor muscles, *B. elegans* lived in a riverine system (Soares et al., 1980; Fulfaro and Perinotto, 1996; Fernandes & Coimbra, 2000; Henriques et al., 2002, 2005; Suárez, 2002; Bertini et al., 2006; Henriques, 2006), then the skull changes and the aquatic habit of this species could be related to the diet

620 changes, as found in other turtles (Dalrymple, 1977; Malvasio et al., 2003; Claude et al., 2004;
621 Pfaller et al., 2011). Once the skull of *B. elegans* comprises all these features, it might probably
622 has gone through changes in diet along ontogeny, from softer to harder aquatic preys. Kischlat
623 (1994) suggested that *B. elegans* might have fed of hard preys and, given the several mollusk and
624 crustacean species described for the Pirapozinho site (Dias-Brito et al., 2001), it might have
625 composed the diet of *B. elegans*. In this context, we agree with Kischlat (1994) and suggest that
626 smaller juveniles individuals might have fed on less hard and small food itens (e.g. snails and
627 small fishes) whereas bigger old specimens fed on harder and larger preys, such as crustaceans
628 and bigger mollusks.

629 **5. Conclusions**

630 As Romano & Azevedo (2007) (for shell material), our data did not show enough
631 morphometrical variation to suggest population differences among our sample. So, we did not
632 have any evidence to disprove that the "Tartaruguito" site is composed by a single population of
633 *B. elegans*. However, it is feasible to assume that different generations of individuals were
634 crowded in this locality by the accumulation of corpses due to several drying events. Since none
635 *B. elegans* hatchling were found in the “Tartaruguito” site until now, it might have been a
636 freshwater foraging area.

637 As regards to the empirical data, the variation and allometric patterns in the bones of the skull,
638 mainly the PA, QJ, SQ, QU, PO, JU, MX, PAL and PT, as well as the loadings of PCA analysis,
639 reflect shape differences in both upper and lower adductor chamber. This could indicate more
640 area attachment and resistance for stronger adductor muscles, which are accompanied by
641 changes in diet during aging, from softer to harder prey, as seen in living turles species.

As regards to the use of images for carrying out morphometrics studies, we conclude that the use of calipers can be replaced by softwares that work on images. ImageJ is an useful tool for this matter. However, one needs to beware of some procedures when taking pictures, in order to avoid methodological flaws in images such as bad focused objects.

Regarding the approaches applied to our data to deal with missing entries in the matrix (i.e. mean value and iterative imputation), both were useful for answering the questions we raised (i.e. the single population hypothesis), though little different results were obtained (few specimens out of 95% ellipse in mean value approach in contrast with none specimen out of ellipse in iterative imputation approach). We recommend the iterative imputation as the most appropriate approach to deal with missing data in paleontological studies on the basis of the statistical assumptions it was developed (a sample-based regression for characters estimation) and the more conservative results, once we have no evidence to assume any specimen as a different species.

Institutional Abbreviations: AMNH – American Museum of Natural History, New York, NY, United States; **LPRP –** Laboratório de Paleontologia da Faculdade de Filosofia, Ciências e Letras de Ribeirão Preto, Universidade de São Paulo, Ribeirão Preto, SP, Brazil; **MN –** Museu Nacional, Universidade Federal do Rio de Janeiro, Rio de Janeiro, RJ, Brazil; **MCT –** Museu de Ciências da Terra, Departamento Nacional de Produção Mineral, Rio de Janeiro, RJ, Brazil; **MCZ –** Museum of Comparative Zoology, Harvard University, Cambridge, MA, United States; **MZSP -** Museu de Zoologia, Universidade de São Paulo, São Paulo, SP, Brazil.

Anatomical abbreviations: PF – prefrontal; **FR –** frontal; **PA –** parietal; **VO –** vomer; **PAL –** palatine; **PT –** pterygoid; **BS –** basisphenoid; **BO –** basioccipital; **MX –** maxilla; **JU –** jugal; **QJ**

– quadratojugal; **QU –** quadrate; **PO –** postorbital; **SQ –** squamosal; **OP –** opisthotic; **CO –** choanal.

Measurements abbreviations: TLS – Total length of skull; **LPF –** Length of prefrontal; **LFR –** Length of frontal; **LPA –** Length of parietal; **LVO –** Length of vomer; **LPAL –** Length of palatine; **LPT –** Length of pterygoid; **LBS –** Length of basisphenoid; **LBO –** Length of basioccipital; **LMX –** Length of maxilla; **LJU –** Length of jugal; **LQJ –** Length of quadratojugal; **LQU –** Length of quadrate; **LPO –** Length of postorbital; **LSQ –** Length of squamosal; **TWS –** Total width of skull; **WPF –** Width of prefrontal; **WFR –** Width of frontal; **WPA –** Width of parietal; **SMX –** Stretch of maxilla; **WVO –** Width of vomer; **WCO –** Width of choanal; **WPAL –** Width of palatine; **WBS –** Width of basisphenoid; **WMX –** Width of maxilla; **WJU –** Width of jugal; **WQJ –** Width of quadratojugal; **WPO –** Width of postorbital; **WOP –** Width of opisthotic.

Acknowledgments

We are grateful to Sergio Azevedo, Deise Henriques, Luciana Carvalho, Lílian Cruz (DGP/MN) and Max Langer (LPRP/USP) for they allowed the loan of the material and visits to collections when necessary. P.S.R.R. thanks the following people and institutions for facilitating access to collections: E. Gaffney, C. Mehling and F. Ippolito (AMNH); R. Cassab and R. Machado (MCT). T.F.M. thanks to Gustavo Oliveira (UFPE) for being part of his monograph committee and for making revisions, suggestions and comments that contributed to this paper and to M. Lambertz (University of Bonn) and C. Mariani for revisions and comments on early versions of the manuscript. Preliminary results of this paper composed the monograph of T.F.M.

6. References

AERTS P, VAN DAMME J, HERREL A. 2001. Intrinsic mechanics and control of fast cranio-cervical movements in aquatic feeding turtles. American Zoologist 41:1299-1310. DOI: dx.doi.org/10.1668/0003-1569(2001)041[1299:IMACOF]2.0.CO;2.

AGUILERA OA. 2004. Tesoros Paleontológicos de Venezuela. Urumaco, Patrimonio Natural de la Humanidad. Editorial Arte: Caracas.

ANQUETIN J. 2012. Reassessment of the phylogenetic interrelationships of basal turtles (Testudinata). Journal of Systematic Paleontology 10(1):3-45. DOI: 10.1080/14772019.2011.558928.

ASTUA D. 2009. Evolution of scapula size and shape in didelphid marsupials (Didelphimorphia: Didelphidae). Evolution 63(9): 2438-2456. DOI: 10.1111/j.1558-5646.2009.00720.x.

BERTINI RJ, SANTUCCI RM, TOLEDO CEV, MENEGAZZO MC. 2006. Taphonomy and depositional history of an Upper Cretaceous turtle-bearing outcrop from the Adamantina Formation, Southwestern São Paulo state. Revista Brasileira de Paleontologia 9(2):181-186.

BHULLAR BAS, MARUGÁN-LOBÓN J, RACIMO F, BEVER GS, ROWE TB, NORELL MA, ABZHANOV A. 2012. Birds have paedomorphic dinosaur skulls. Nature 0. DOI: 10.1038/nature11146.

BURNELL A, COLLINS S, YOUNG BA. 2012. Vertebral morphometrics in *Varanus.* Bulletin de la Societe Geologique de France 183(2): 151-158.

CADENA EA, BLOCH JI, JARAMILLO CA. 2010. New podocnemidid turtle (Testudines: Pleurodira) from the Middle-Upper Paleocene of South America. Journal of Vertebrate Paleontology 30(2):367-382. DOI: dx.doi.org/10.1080/02724631003621946.

CADENA EA, BLOCH JI, JARAMILLO CA. 2012. New bothremydid turtle (Testudines, Pleurodira) from the Paleocene of Northeastern Colombia. Journal of Paleontology 86(4):688-698. DOI: dx.doi.org/10.1666/11-128R1.1.

CADENA EA, KSEPKA DT, JARAMILLO CA, BLOCH JI. 2012. New pelomedusoid turtles from the late Paleocene Cerrejón Formation of Colombia and their implications for phylogeny and body size evolution. Journal of Systematic Paleontology 10(2):313-331. DOI: dx.doi.org/10.1080/14772019.2011.569031.

CAMPOS DA, OLIVEIRA GR, FIGUEIREDO RG, RIFF D, AZEVEDO SAK, CARVALHO LB, KELLNER AWA. 2011. On a new peirosaurid crocodyliform from the Upper Cretaceous, Bauru Group, southeastern Brazil. Anais da Academia Brasileira de Ciências 83(1):317-327. DOI: dx.doi.org/10.1590/S0001-37652011000100020.

718 CLAUDE J, PRITCHARD PCH, TONG H, PARADIS E, AUFFRAY JC. 2004. Ecological
719 correlates and evolutionary divergence in the skull of turtles: a geometric mophometric
720 assessment. Systematic Biology 53(6):933-962. DOI: 10.1080/10635150490889498.

721 CONGDON JD, NAGLE RD, KINNEY OM, SELS RCVL, QUINTER T, TINKLE DW. 2003.
722 Testing hypotheses of aging in long-lived painted turtles (Chrysemys picta). Experimental
723 Gerontology 38:765-772.

724 CORRUCCINI RS. 1983. Principal Components for allometric analysis. American Journal of
725 Physical Anthropology 60: 451-453.

726 COSTA HC, MOURA MR, FEIO RN. 2013. Taxonomic revision of *Drymoluber* Amaral, 1930
727 (Serpentes: Colubridae). Zootaxa 3716(3): 349-394. DOI: dx.doi.org/10.11646/zootaxa.3716.3.3.

728 DALRYMPLE GH. 1977. Intraspecific variation in the cranial feeding mechanism of turtles of
729 the genus *Trionyx* (Reptilia, Testudines, Trionychidae). Journal of Herpetology 11(3):255-285.
730 DOI: 10.2307/1563241.

731 DEPECKER M, RENOUS S, PENIN X, BERGE C. 2005. Procrustes analysis: a tool to
732 understand shape changes of the humerus in turtles (Chelonii). Comptes Rendus Palevol 5: 509-
733 518.

734 DEPECKER M, BERGE C, PENIN X, RENOUS S. 2006. Geometric morphometrics of the
735 shoulder girdle in extant turtles (Chelonii). Journal of Anatomy 208: 35-45.

736 DE BROIN F. 1991. Fossil turtles from Bolivia. In: Suarez-Soruco R. *Fossiles y facies de*
737 *Bolívia – Vol. I Vertebrados*. Revista Técnica de YPFB, 12(3-4): 509-527.

738 DE LA FUENTE MS, STERLI J, MANIEL I. 2014. Origin, evolution and biogeographic
739 history of South American turtles. Springer Earth System Sciences.

740 FABRE AC, CORNETTE R, PERRARD A, BOYER DM, PRASAD GR, HOOKER JJ,
741 GOSWAMI A. 2014. A three-dimensional morphometric analysis of the locomotory ecology of
742 *Deccanolestes*, a eutherian mammal from the Late Cretaceous of India. Journal of Vertebrate
743 Paleontology 34(1): 146-156.

744 FERNANDES LB, COIMBRA AM. 2000. Revisão estratigráfica da parte oriental da Bacia
745 Bauru (Neocretáceo). Revista Brasileira de Geociências 30(4):717-728.

746 FERREIRA GS, RINCÓN AD, SOLÓRZANO A, LANGER MC. 2015. The last marine
747 pelomedusoids (Testudines: Pleurodira): a new species of *Bairdemys* and the paleoecology of
748 Stereogyina. PeerJ 3:e1063. DOI: 10.7717/peerj.1063.

749 FRANÇA MAG, LANGER MC. 2005. A new freshwater turtle (Reptilia, Pleurodira,
750 Podocnemidae) from the Upper Cretaceous (Maastrichtian) of Minas Gerais, Brazil.
751 Geodiversitas 27: 391-411.

752 FRAZZETTA TH. 1968. Adaptative problems and possibilities in the temporal fenestration of
753 tetrapod skulls. Journal of Morphology 125:145-157.

754 FULFARO VJ, PERINOTTO JAJ. 1996. A Bacia Bauru: estado da arte. Boletim do Quarto
755 Simpósio sobre o Cretáceo do Brasil, UNESP, Rio Claro, SP: 297-303.

756 FUTUYMA DJ. 1993. *Biologia evolutiva*. 2 ed. Ribeirão Preto: FUNPEC-RP.

757 GAFFNEY ES. 1972. An Illustred Glossary of Turtle Skull Nomeclature. American Museum
758 Novitates 2486:33pp.

759 GAFFNEY ES. 1975. A phylogeny and classification of the higher categories of turtles. Bulletin
760 of the Americam Museum of Natural History 155(5):387-436.

761 GAFFNEY ES. 1979. Comparative Cranial Morphology of Recent and Fossil Turtles. Bulletin of
762 the American Museum of Natural History 164(2):65-376.

763 GAFFNEY ES, KRAUSE DW. 2011. *Sokatra*, a new side-necked turtle (Late Cretaceous,
764 Madagascar) and the diversification of the main groups of Pelomedusoides. American Museum
765 Novitates 3728:28pp. DOI: dx.doi.org/10.1206/3728.2.

766 GAFFNEY ES, MEYLAN PA, WOOD RC, SIMONS E, CAMPOS DA. 2011. Evolution of the
767 side-necked turtles: the family Podcnemididae. Bulletin of the American Museum of Natural
768 History 350: 237pp. DOI: dx.doi.org/10.1206/350.1.

769 GAFFNEY ES., MEYLAN PA, WYSS AR. 1991. A computer assisted analysis of the
770 relationships of the higher categories of turtles. Cladistics 7:313-335. DOI: 10.1111/j.1096-
771 0031.1991.tb00041.x.

772 GAFFNEY ES, SCHEYER TM, JOHNSON KG, BOCQUENTIN J, AGUILERA OA. 2008.
773 Two new species of the side necked turtle genus, *Bairdemys* (Pleurodira, Podocnemididae), from
774 the Miocene of Venezuela. Palaontoloqische Zeitschrift 82(2):209-229.

775 GAFFNEY ES, TONG H, MEYLAN PA. 2006. Evolution of the sidenecked turtles: the families
776 Bothremydidae, Euraxemydidae and Araripemydidae. Bulletin of the American Museum of
777 Natural History 300:698pp. DOI: dx.doi.org/10.1206/0003-
778 0090(2006)300[1:EOTSTT]2.0.CO;2.

779 GOULD SJ. 1966. Allometry and size in ontogeny and phylogeny. Biological Reviews 41:587-
780 640. DOI: 10.1111/j.1469-185X.1966.tb01624.x.

781 GOULD SJ. 1979. An allometric interpretation of species-area curver: the meaning of the
782 coefficient. The American Naturalist 114(3):335-343.

783 HAMMER Ø, HARPER DAT, RYAN PD. 2001. Past: Palentological Statistics software
784 package for education and data analysis. Palaeontologia Electronica 4(1):9pp.

785 HAMMER Ø, HARPER DAT. 2006. *Paleontological Data Analysis*. Blackwell.

786 HENNIG, W. 1966. *Phylogenetic Systematics*. Urbana: University of Illinois Press.

787 HENRIQUES DDR. 2006. Sítio fossilífero de Pirapozinho: estudo de aspectos taxonômicos
788 através da análise básica e do exame de tomografia computadorizada. D. Phil. Thesis. Museu
789 Nacional – Universidade Federal do Rio de Janeiro.

790 HENRIQUES DDR, SUÁREZ JM, AZEVEDO SAK, CAPILLA R, CARVALHO LB. 2002. A
791 brief note on the paleofauna of "Tartaruguito" site, Adamantina Formation, Bauru Group, Brazil.
792 Anais da Academia Brasileira de Ciências 74(2): 366.

793 HENRIQUES DDR, AZEVEDO SAK, CAPILLA R. SUÁREZ JM. 2005. The Pirapozinho Site
794 – a taphofacies study. Journal of Vertebrate Paleontology 25:69A.

795 HERREL A, O'REILLY JC, RICHMOND AM. 2002. Evolution of bite performance in turtles.
796 Journal of Evolutionary Biology 15:1083-1094. DOI: 10.1046/j.1420-9101.2002.00459.x.

797 HUXLEY JS. 1950. Relative growth and form transformation. Proceedings of the Royal Society
798 of London B 137:465-469. DOI: 10.1098/rspb.1950.0055.

799 HUXLEY JS, TEISSIER G. 1936. Terminology of Relative Growth. Nature 137:780-781. DOI:
800 10.1038/137780b0.

801 ILIN A, RAIKO T. 2010. Practical approaches to Principal Components Analysis in the presence
802 of missing values. Journal of Machine Learning Research 11:1957-2000.

803 JARAMILLO CA, BAYONA G, PARDO-TRUJILLO A, RUEDA M, TORRES V,
804 HARRINGTON GJ, MORA G. 2007. The palynology of the Cerrejón formation (Upper
805 Paleocene) of northern Colombia. Palynology 31(1):153-189. DOI:
806 10.1080/01916122.2007.9989641.

807 JOLICOEUR P, MOSIMANN JE. 1960. Size and shape variation in the painted turtle: a
808 Principal Component Analysis. Growth 24: 339-354.

809 JONES MEH, WERNEBURG I, CURTIS N, PENROSE R, O'HIGGINS P, FAGAN MJ,
810 EVANS SE. 2012. The head and neck anatomy of sea turtles (Cryptodira: Chelonioidea) and
811 skull shape in Testudines. PloS ONE 7(11):e47852. DOI: 10.1371/journal.pone.0047852. DOI:
812 10.1371/journal.pone.0047852.

JOYCE WG. 2007. Phylogenetic relationships of Mesozoic turtles. Bulletin of Peabody Museum of Natural History 48(1):3-102. DOI: dx.doi.org/10.3374/0079-032X(2007)48[3:PROMT]2.0.CO;2.

KISCHLAT EE. 1994. Observações sobre *Podocnemis elegans* Suaréz (Chelonii, Pleurodira, Podocnemididae) do Neocretáceo do Brasil. Acta Geologica Leopoldensia, 39: 345-351.

KISCHLAT EE, BARBARENA, MC, TIMM, LL. 1994. Considerações sobre a queloniofauna do Grupo Bauru, Neocretáceo do Brasil [Boletim do Simpósio sobre o Cretáceo do Brasil, Rio Claro: Universidade Estadual Paulista. 105-107.

KLINGER RC, MUSICK JA. 1995. Age and growth of loggerhead turtles (*Caretta caretta*) from Chesapeake Bay. Copeia 1:204-209.

KRZANOWSKI WJ. 1979. Between-Groups comparison of Principal Components. Journal of the American Statistical Association 74: 703-707.

KRZANOWSKI WJ. 1979. Between-Groups comparison of Principal Components – some sampling results. Journal of Statistical Computation Simulation 15: 141-154.

LEMELL P, BEISSER CJ, WEISGRAM J. 2000. Morphology and function of the feeding apparatus of *Pelusios castaneus* (Chelonia; Pleurodira). Journal of Morphology 244:127-135. DOI: 10.1002/(SICI)1097-4687(200005)244:2<127::AID-JMOR3>3.0.CO;2-U.

LEMELL P, LEMELL C, SNELDERWAARD P, GUMPENBERGER M, WOCHESLÄNDER R, WEISGRAM J. 2002. Feeding patterns in *Chelus fimbriatus* (Pleurodira: Chelidae). The Journal of Experimental Biology 205:1495-1506. PubMed: 11976360.

LYSON TR, JOYCE WG. 2009. A new species of *Palatobaena* (Testudines: Baenidae) and a maximum parsimony and bayesian phylogenetic analysis of Baenidae. Journal of Paleontology 83(3): 457-470. DOI: dx.doi.org/10.1666/08-172.1.

LYSON TR, JOYCE WG. 2010. A new baenid turtle from the Upper Cretaceous (Maastrichtian) Hell Creek Formation of North Dakota and a preliminary taxonomic review of Cretaceous Baenidae. Journal of Vertebrate Paleontology 30(2):394-402. DOI: dx.doi.org/10.1080/02724631003618389.

MARIANI TF, ROMANO PSR. 2014. Quando não podemos usar paquímetro: ImageJ como ferramenta para obtenção de dados morfométricos em fósseis [abstract no. 61]. Boletim de Resumos do IX Simpósio Brasileiro de Paleontologia de Vertebrados.

MALVASIO A, SOUZA AM., MOLINA FB, SAMPAIO FA. 2003. Comportamento e preferência alimentar em *Podocnemis expansa* (Schweigger), *P. unifilis* (Troschel) e *P. sextubeculata* (Cornalia) em cativeiro (Testudines, Pelomedusidae). Revista Brasileira de Zoologia, 20(1):161-168. DOI: dx.doi.org/10.1590/S0101-81752003000100021.

MINGOTI SA. 2013. Análise de dados através de métodos de estatística multivariada: uma abordagem aplicada. Editora UFMG.

NORELL MA, WHEELER WC. 2003. Missing entry replacement data analysis: a replacement approach to dealing with missing data in paleontological and total evidence data sets. Journal of Vertebrate Paleontology 23(2): 275-283.

OLIVEIRA GR. 2011. Filogenia e descrição de novos Podocnemididae (Pleurodira: Pelomedusoides). D. Phil. Thesis. Museu Nacional – Universidade Federal do Rio de Janeiro.

OLIVEIRA GR, ROMANO PSR. 2007. Histórico dos achados de tartarugas fósseis do Brasil. Arquivos do Museu Nacional 65(1):113-133.

PARSONS TS, WILLIAMS EE. 1961. Two Jurassic turtle skulls: a morphological study. Bulletin of the Museum of Comparative Zoology 125(3):41-107.

PERES-NETO PR, JACKSON DA, SOMERS KM. 2003. Giving meaningful interpretation to ordination axes: assessing loading significance in Principal Component Analysis. Ecology 84(9): 2347-2363.

PFALLER JB, GIGNAC PM, ERICKSON GM. 2011. Ontogenetic changes in jaw-muscle architecture facilitate durophagy in turtle *Sternotherus minor*. Journal of Experimental Biology 214:1655-1667. DOI: 10.1242/jeb.048090.

PFALLER JB, HERRERA ND, GIGNAC PM, ERICKSON GM. 2010. Ontogenetic scaling of cranial morphology and bite-force generation in the loggerhead musk turtle. Journal of Zoology 280:280-289. DOI: 10.1111/j.1469-7998.2009.00660.x.

PRICE IL. 1953. Os quelônios da Formação Bauru, Cretáceo terrestre do Brasil meridional. Rio de Janeiro: Departamento Nacional de Produção Mineral/Divisão de Geologia e Mineralogia, 34pp. (Boletim 147).

RABI M, ZHOU CF, WINGS O, GE S, JOYCE WG. 2013. A new xinjiangchelyid turtle from the Middle Jurassic of Xinjiang, China and the evolution of the basipterygoid process in Mesozoic turtles. BMC Evolutionary Biology 13:203. DOI: 10.1186/1471-2148-13-203.

RASBAND WS. 1997. ImageJ, U.S.National Institutes of Health, Bethesda, Maryland, USA. *Avaiable at* www.imagej.nih.gov/ij/. 1997-2012.

RIEPPEL O. 1993. Patterns of Diversity in the Reptilian Skull. In: Hanken J, Hall BK, *The Skull, Vol. 2: Patterns of Structural and Systematic Diversity*. Chicago: The University of Chicago Press, 344-390.

RIFF D, ROMANO PSR, OLIVEIRA GR, AGUILERA OA. 2010. Neogene crocodile and turtle fauna in northern South America. In: Hoorn C, Wesselingh FP ed. *Amazonia, Landscape and Species Evolution: A Look into the Past*. Wiley-Blackwell Publishing. 259-280.

ROMANO PSR. 2008. An unusual specimen of *Bauruemys elegans* and its implication for the taxonomy of the side-necked turtles from Bauru Basin (Upper Cretaceous of Brazil). Journal of Vertebrate Paleontology 28 (suppl. 3): 133A-134A.

ROMANO PSR. 2010. Evolução do crânio em Pelomedusoides (Testudines, Pleurodira). D. Phil. Thesis. Museu Nacional – Universidade Federal do Rio de Janeiro.

ROMANO PSR, AZEVEDO SAK. 2006. Are extant podocnemidid turtles relicts of a widespread Cretaceous ancestor? South American Journal of Herpetology 1(3):175-184. DOI: 10.2994/1808-9798(2006)1[175:AEPTRO]2.0.CO;2.

ROMANO PSR, AZEVEDO SAK. 2007. Morphometric analysis of the Upper Cretaceous brazilian side-necked turtle *Bauruemys elegans* (Suárez, 1969) (Pleurodira, Podocnemididae). Arquivos do Museu Nacional 65(4):395-402.

ROMANO PSR, GALLO V, RAMOS RRC, ANTONIOLI L. 2014. *Atolchelys lepida*, a new side-necked turtle from the Early Cretaceous of Brazil and the age of Crown-Pleurodira. Biology Letters 10: 20140290. DOI: 10.1098/rsbl.2014.0290.

ROMANO PSR, OLIVEIRA GR, AZEVEDO SAK, CAMPOS DA. 2009. Lumping the podocnemidid turtles species from Bauru Basin (Upper Cretaceous of Southeastern of Brazil) [abstract no. 38]. Gaffney Turtle Symposium Abstract Volume: 141-152.

ROMANO PSR, OLIVEIRA GR, AZEVEDO SAK, KELLNER AWA, CAMPOS DA. 2013. New information about Pelomedusoides (Testudines: Pleurodira) from the Cretaceous of Brazil. In: Brinkman D, Holroyd P, Gardner J, ed. *Morphology and evolution of turtles.* Vertebrate Paleobiology and Paleoanthropology Series. Dordrecht, The Netherlands: Springer, 261-275.

SÁNCHEZ-VILLAGRA MR, AGUILERA OA. 2006. Neogene Vertebrates from Urumaco, Falcón State, Venezuela: Diversity and Significance. Journal of Systematic Palaeontology 4(3):213-220. DOI: 10.1017/S1477201906001829.

SÁNCHEZ-VILLAGRA MR, WINKLER JD. 2006. Cranial variation in *Bairdemys* turtles (Podocnemididae: Miocene of the Caribbean region) and description of new material from Urumaco, Venezuela. Journal of Systematic Paleontology 4(3):241-253. DOI: 10.1017/S1477201906001891.

SCHUMACHER GH. 1973. The head muscles and hyolaryngeal skeleton of turtles and crocodilians. In: Gans C, *Biology of Reptilia, vol. 4: Morphology D*. London: Academic Press, 101-199.

SHINE RS, IVERSON JB. 1995. Patterns of survival, growth and maturation in turtles. Oikos 72(3):343-348. DOI: 10.2307/3546119.

SMITH KK. 1993. The form of the feeding apparatus in terrestrial vertebrates: studies of adaptation and constraint. In: Hanken J, Hall BK, *The Skull, Vol. 3:Functional and Evolutionary Mechanisms.* Chicago: The University of Chicago Press, 150-196.

SOARES PC, LANDIM PMB, FULFARO VJ, NETO AFS. 1980. Ensaio de caracterização estratigráfica do Cretáceo no estado de São Paulo: Grupo Bauru. Revista Brasileira de Geociências 10:177-185.

SOMERS KM. 1986. Multivariate allometry and removal of size with principal components analysis. Systematic Zoology 35(3): 359-368.

SOMERS KM. 1989. Allometry, Isometry and Shape in Principal Components Analysis. Systematic Zoology 38(2):169-173.

STERLI J, DE LA FUENTE MS. 2010. Anatomy of *Condorchelys antiqua* Sterli, 2008, and the origin of the modern jaw closure mechanism in turtles. Journal of Vertebrate Paleontology 30(2):351-366. DOI: 10.1080/02724631003617597.

STERLI J, MÜLLER J, ANQUETIN J, HILGER A. 2010. The parabasisphenoid complex in Mesozoic turtles and the evolution of the testudinate basicranium. Canadian Journal of Earth Sciences 47:1337-1346. DOI: 10.2307/3546119.

STRAUSS RE, ATANASSOV MN, OLIVEIRA JA. 2003. Evaluation of the principal-component and expectation-maximization methods for estimating missing data in morphometric studies. Journal of Vertebrate Paleontology 23(2): 284-296.

SUÁREZ, JM. 1969a. Um nôvo quelônio fóssil da Formação Baurú [abstract no. 153]. Comunicações do Congresso Brasileiro de Geologia, Salvador: Boletim Especial, Salvador, 1:87-89.

SUÁREZ, JM. 1969b. Um quelônio da Formação Bauru. Boletim da Faculdade de Filosofia, Ciências e Letras de Presidente Prudente 2:35-54.

SUÁREZ, JM. 1969c. Um quelônio da Formação Bauru [abstract no. 12]. Anais do Congresso Brasileiro de Geologia, Salvador. 167-176.

SUÁREZ JM. 2002. Sítio fossilífero de Pirapozinho, SP – Extraordinário depósito de quelônios do Cretáceo. In: Schobbenhaus C, Campos DA, Queiroz ET, Winge M, Berbert-Born M. *Sítio geológicos e paleontológicos do Brasil*.

SUNDBERG P. 1989. Shape and size-contrained Principal Components Analysis. Systematic Zoology 38(2): 166-168.

VAN DAMME J, AERTS P. 1997. Kinematics and functional morphology of aquatic feeding in australian snake-necked turtles (Pleurodira; *Chelodina*). Journal of Morphology 233:113-125. DOI: 10.1002/(SICI)1097-4687(199708)233:2<127::AID-JMOR4>3.0.CO;2-3.

WERNEBURG I. 2011. The cranial musculature of turtles. Palaentologia eletronica 14(2):99p; palaeo-electronica.org/2011_2/254/index.html.

WERNEBURG I. 2012. Temporal bone arrangements in turtles: an overview. Journal of Experimental Zoology 318:235-249. DOI: 10.1002/jez.b.22450.

WERNEBURG I. 2013. The tendinous framework in the temporal skull region of turtles and considerations about its morphological implications in amniotes: a review. Zoological Science 30:141-153. DOI: 10.2108/zsj.30.141.

WERNEBURG I, WILSON LAB, PARR WCH, JOYCE WG. 2014. Evolution of neck vertebral shape and neck retraction at the transition to Modern Turtles: an integrated geometric morphometric approach. Systematic Biology 0(0): 1-18. DOI: 10.1093/sysbio/syu072.

WINGS O, RABI M, SCHNEIDER JW, SCHWERMANN L, SUN G, ZHOU CF, JOYCE WG. 2012. An enormous Jurassic turtle bone bed from the Turpan Basin of Xinjiang, China. Naturwissenschaften 99:925-935. DOI: 10.1007/s00114-012-0974-5.

1

Fossil turtle localities in Bauru Basin

Lithostratigraphical map of the oriental part of the Bauru Basin showing the fossil turtle localities (municipalities). Turtle species are: **1.** *Cambaremys langertoni* (*incertae sedis*), *Pricemys caieira* and *Peiropemys mezzalirai*; **2.** *Roxochelys harrisi* (*nomem dubium*); **3.** *Bauruemys brasiliensis* (*nomem dubium*) and Testudines indet.; **4.** Testudines indet.; **5.** Testudines indet.; **6.** *B. brasiliensis* and *Roxochelys wanderleyi*; **7.** Testudines indet.; **8.** Testudines indet.; **9.** Podocnemididae indet.; **10.** *Roxochelys* sp. and *R. wanderleyi*; **11.** *B. elegans*. Abbreviations: **GO,** Goiás State; **MG,** Minas Gerais State; **MS,** Mato Grosso do Sul State; **PR,** Paraná State; **SP,** São Paulo State. Scale bar in Km. Map modified from Romano et al. (2009); geology following Fernandes (2004); taxonomy status of species following Romano et al. (2013).

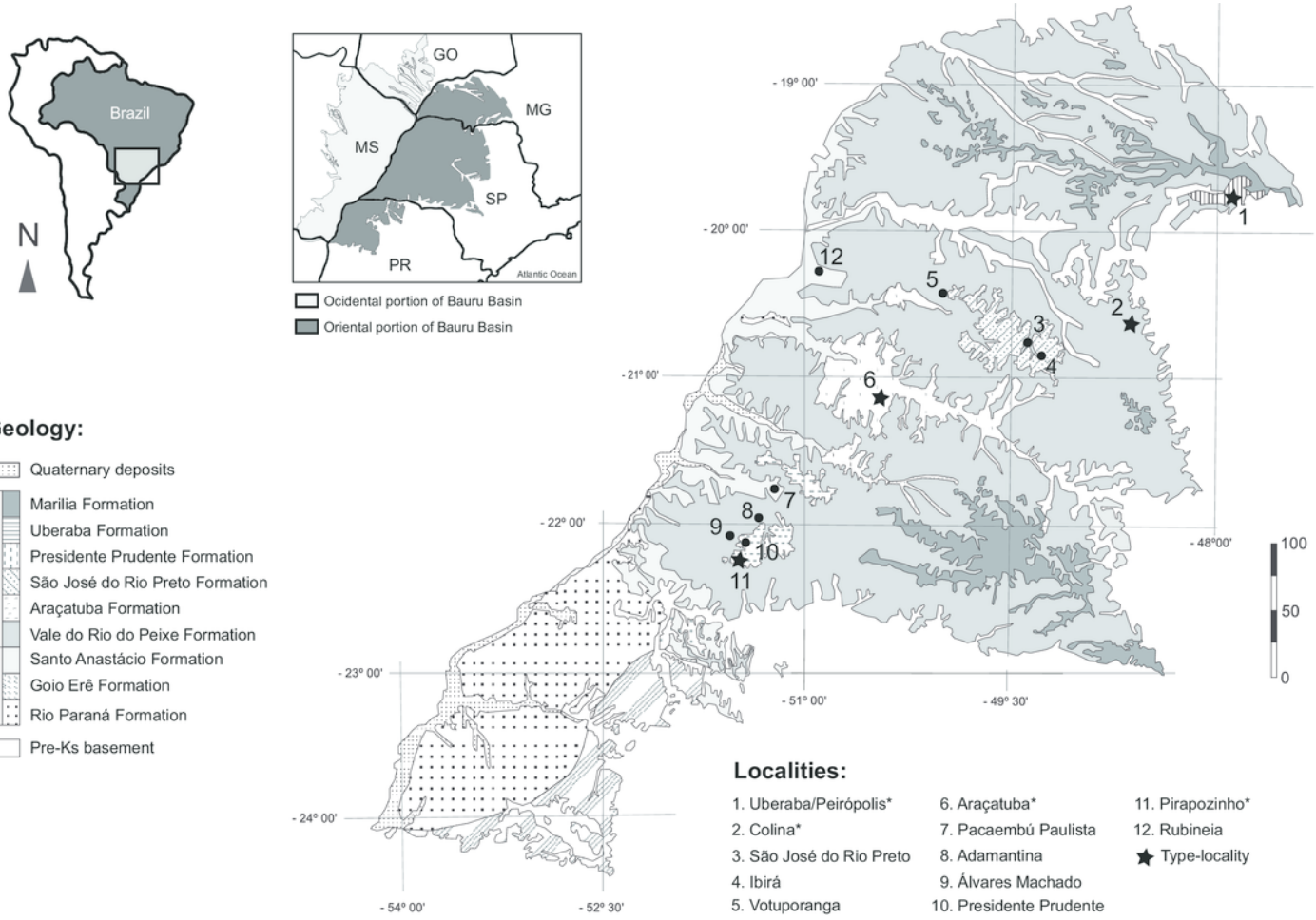
Brazil
N
GO
MG
MS
SP
PR
Atlantic Ocean
Ocidental portion of Bauru Basin
Oriental portion of Bauru Basin
Geology:
Quaternary deposits
Bauru Group
Marilia Formation
Uberaba Formation
Presidente Prudente Formation
São José do Rio Preto Formation
Araçatuba Formation
Vale do Rio do Peixe Formation
Caiuá Group
Santo Anastácio Formation
Goio Erê Formation
Rio Paraná Formation
Pre-Ks basement
- 19° 00'
- 20° 00'
- 21° 00'
- 22° 00'
- 23° 00'
- 24° 00'
- 54° 00'
- 52° 30'
- 51° 00'
- 49° 30'
- 48°00'
100
50
0
Localities:
1. Uberaba/Peirópolis*
2. Colina*
3. São José do Rio Preto
4. Ibirá
5. Votuporanga
6. Araçatuba*
7. Pacaembú Paulista
8. Adamantina
9. Álvares Machado
10. Presidente Prudente
11. Pirapozinho*
12. Rubineia
Type-locality

2

Image of landmarks used as references for taking measurements.

Skull of *Bauruemys elegans* in (A) dorsal, (B) ventral and (C) right lateral views showing the anatomical nomenclature and the 39 landmarks used for morphometrics analysis. All measurements were taken between two landmarks (see table 2 for vectors description). **Abbreviations: bo,** basioccipital; **bs,** basisphenoid; **ex,** exoccipital; **fpp,** foramen palatinum posterius; **fr,** frontal; **ju,** jugal; **mx,** maxilla; **op,** opisthotic; **pa,** parietal; **pal,** palatine; **pf,** prefrontal; **pm,** premaxilla; **po,** postorbital; **pt,** pterygoid; **ptp,** processus trochlearis pterygoidei; **qj,** quadratojugal; **qu,** quadrate; **sq,** squamosal; **so,** supraoccipital; **vo,** vomer. Skull lineation from Gaffney et al. (2011, p.72).

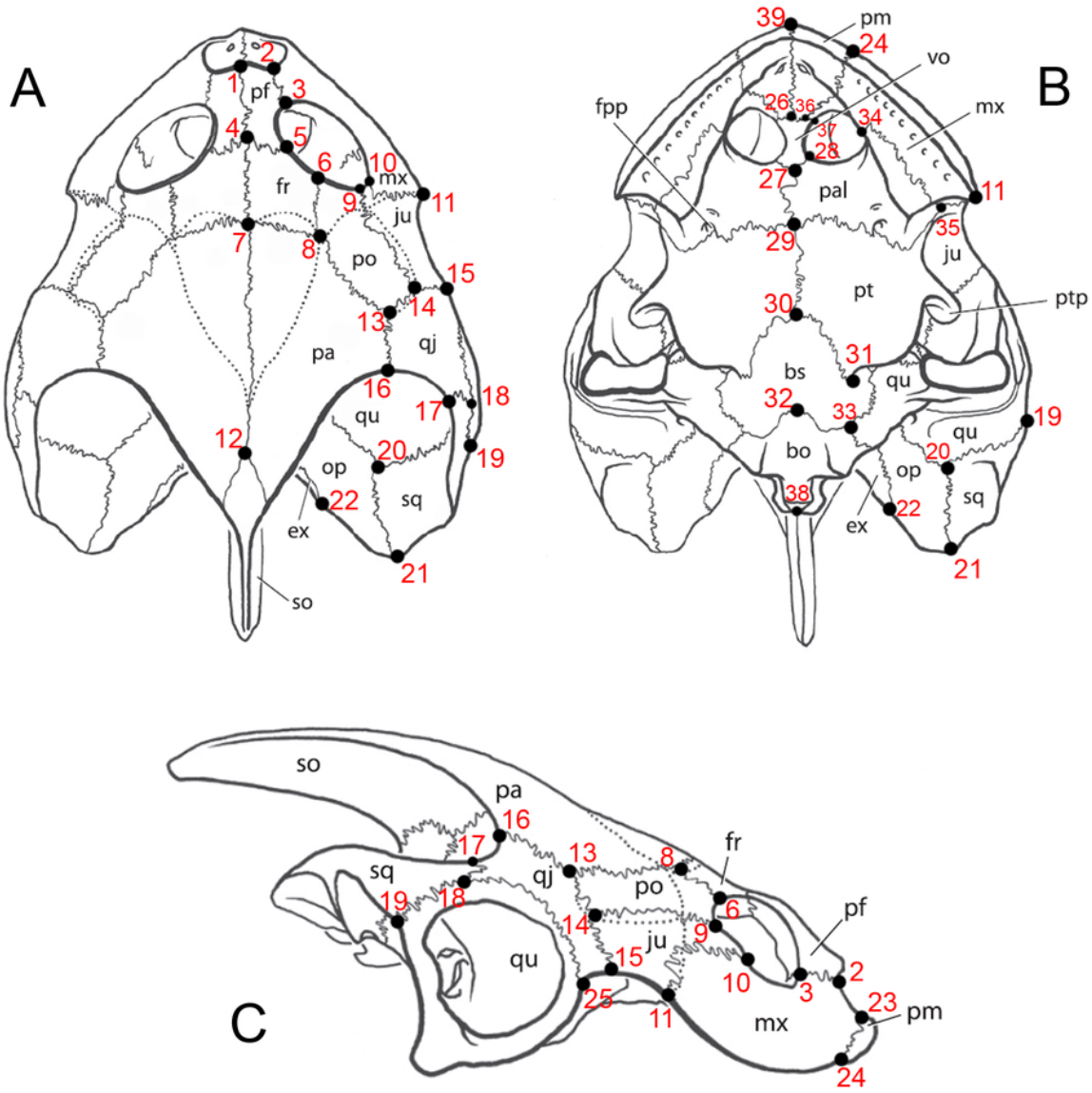
A
1
2
pf
3
4
5
6
10
mx
fr
9
11
ju
7
8
po
15
14
13
qj
pa
16
18
qu
17
12
20
19
op
22
sq
ex
21
so
B
39
pm
24
vo
fpp
26
36
mx
34
37
28
27
pal
11
29
35
ju
pt
ptp
30
31
bs
qu
32
33
19
qu
bo
20
op
38
sq
ex
22
21
C
so
pa
16
17
13
8
fr
sq
qj
po
19
18
6
pf
14
9
ju
qu
15
10
2
25
3
23
pm
11
mx
24

3

Allometric graphics: part 1.

Allometries of *Bauruemys elegans* skull bones: (A) lenght of parietal (LPA), (B) lenght of maxilla (LMX), (C), lenght of jugal (LJU), (D) lenght of quadrate (LQU), (E) lenght of squamosal (LSQ), (F) lenght of pterygoid (LPT), (G) lenght of postorbital (LPO), (H) stretch of maxilla (SMX), (I) width of quadratojugal (WQJ) (J) and width of parietal (WPA). Angular coefficient (a) and coefficient of correlation (r) are shown. **Abbreviations: TLS,** total lenght of the skull; **TWS,** total width of the skull.

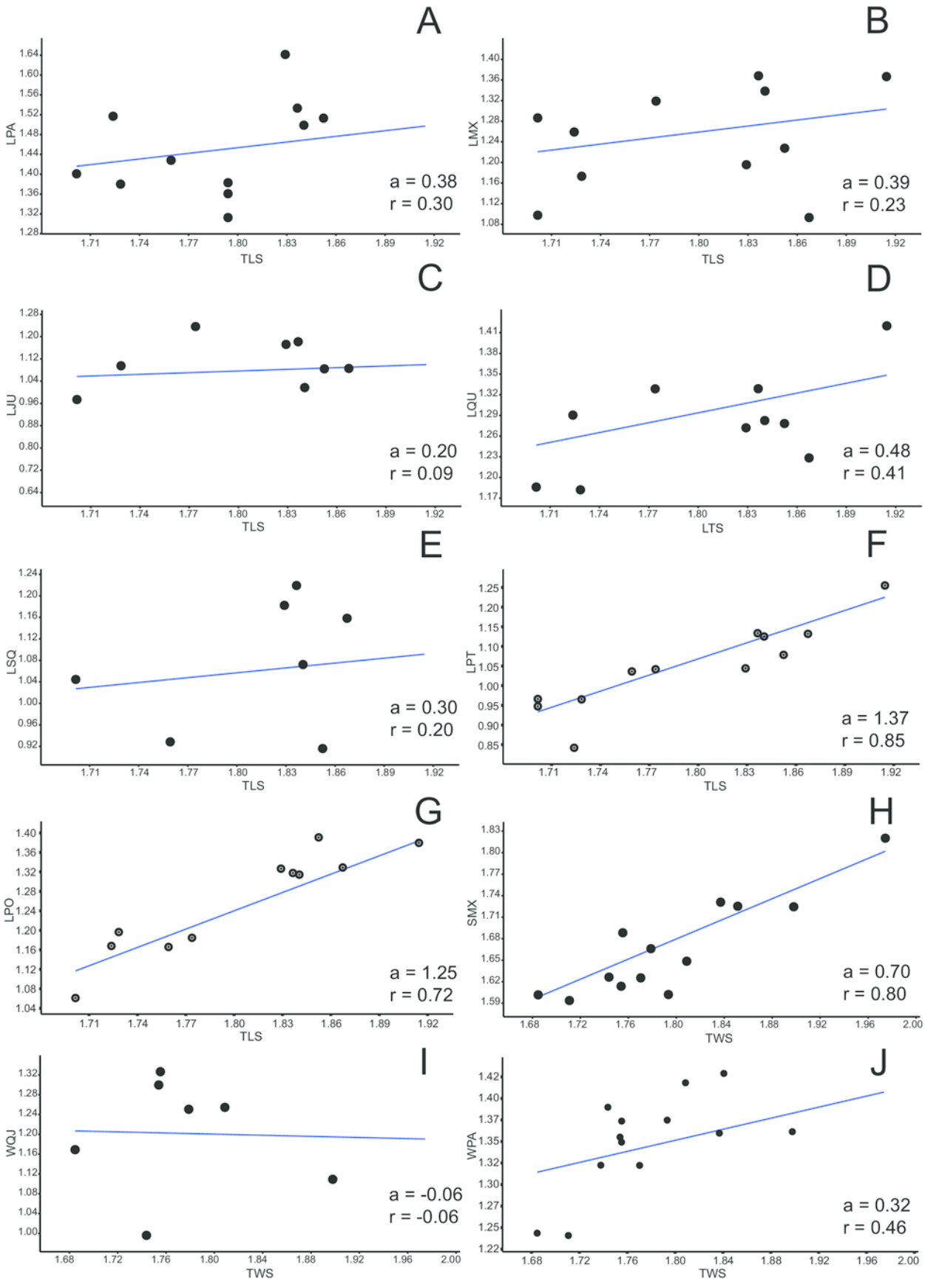
A
LPA
TLS
a = 0.38
r = 0.30
B
LMX
TLS
a = 0.39
r = 0.23
C
LJU
TLS
a = 0.20
r = 0.09
D
LQU
LTS
a = 0.48
r = 0.41
E
LSQ
TLS
a = 0.30
r = 0.20
F
LPT
TLS
a = 1.37
r = 0.85
G
LPO
TLS
a = 1.25
r = 0.72
H
SMX
TWS
a = 0.70
r = 0.80
I
WQJ
TWS
a = -0.06
r = -0.06
J
WPA
TWS
a = 0.32
r = 0.46

4

Allometric graphics: part 2.

Allometries of *Bauruemys elegans* skull bones: (A) lenght of basioccipital (LBO), (B) lenght of basisphenoid (LBS), (C), lenght of palatine (LPAL), (D) lenght of frontal (LFR), (E) lenght of prefrontal (LPF), (F) lenght of quadratojugal (LQJ), (G) lenght of vomer (LVO), (H) width of postorbital (WPO), (I) width of opisthotic (WOP) (J) and width of choanal (WCO). Angular coefficient (a) and coefficient of correlation (r) are shown. **Abbreviations: TLS,** total lenght of the skull; **TWS,** total width of the skull.

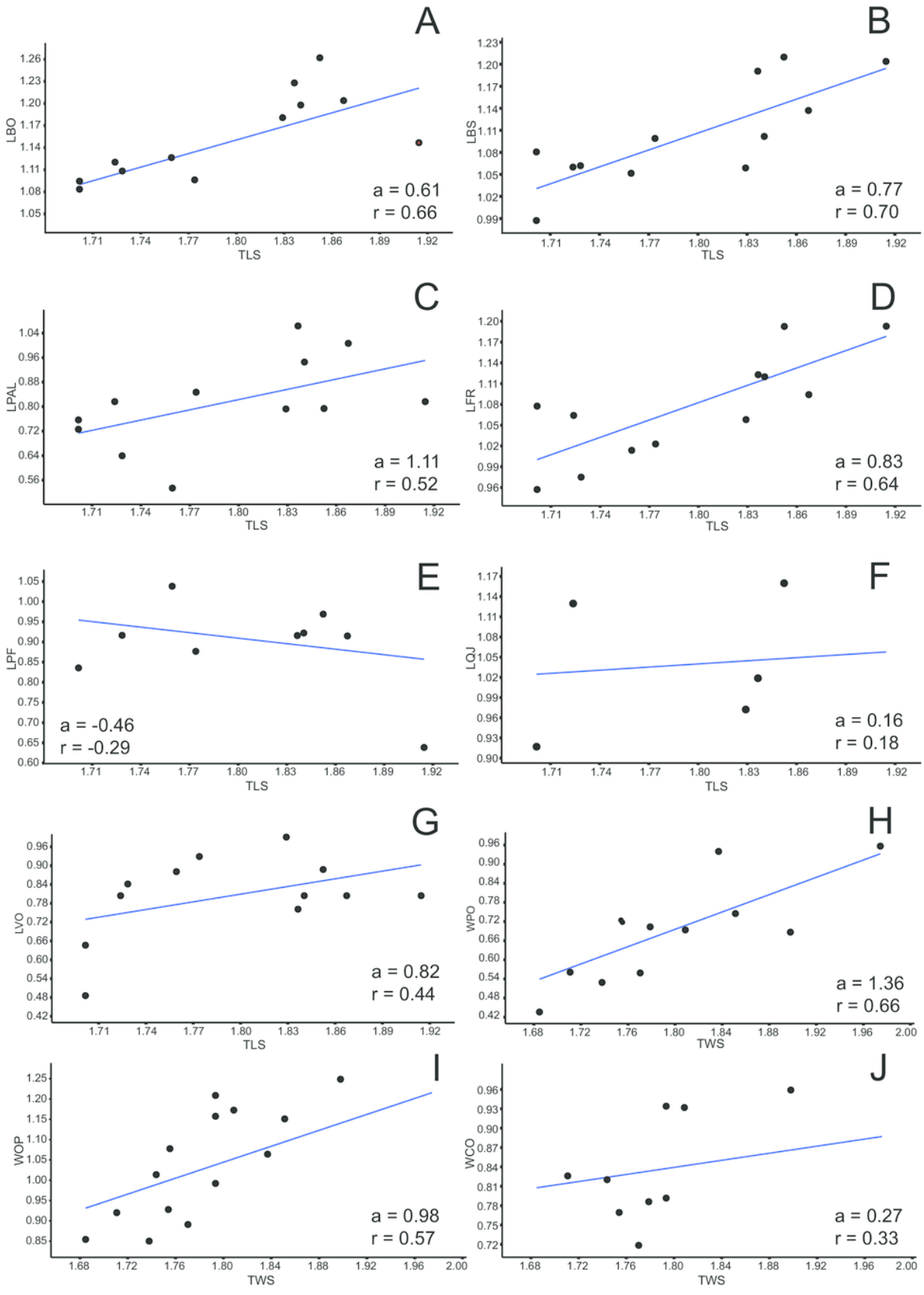
A
LBO
TLS
a = 0.61
r = 0.66
B
LBS
TLS
a = 0.77
r = 0.70
C
LPAL
TLS
a = 1.11
r = 0.52
D
LFR
TLS
a = 0.83
r = 0.64
E
LPF
TLS
a = -0.46
r = -0.29
F
LQJ
TLS
a = 0.16
r = 0.18
G
LVO
TLS
a = 0.82
r = 0.44
H
WPO
TWS
a = 1.36
r = 0.66
I
WOP
TWS
a = 0.98
r = 0.57
J
WCO
TWS
a = 0.27
r = 0.33

5

Allometric graphics: part 3.

Allometries of *Bauruemys elegans* skull bones: (A) width of maxilla (WMX), (B) width of jugal (WJU), (C), width of frontal (WFR), (D) width of prefrontal (WPF), (E) width of basisphenoid (WBS), (F) width of palatine (WPAL) and (G) width of vomer (WVO). Angular coefficient (a) and coefficient of correlation (r) are shown. **Abbreviations: TWS,** total width of the skull.

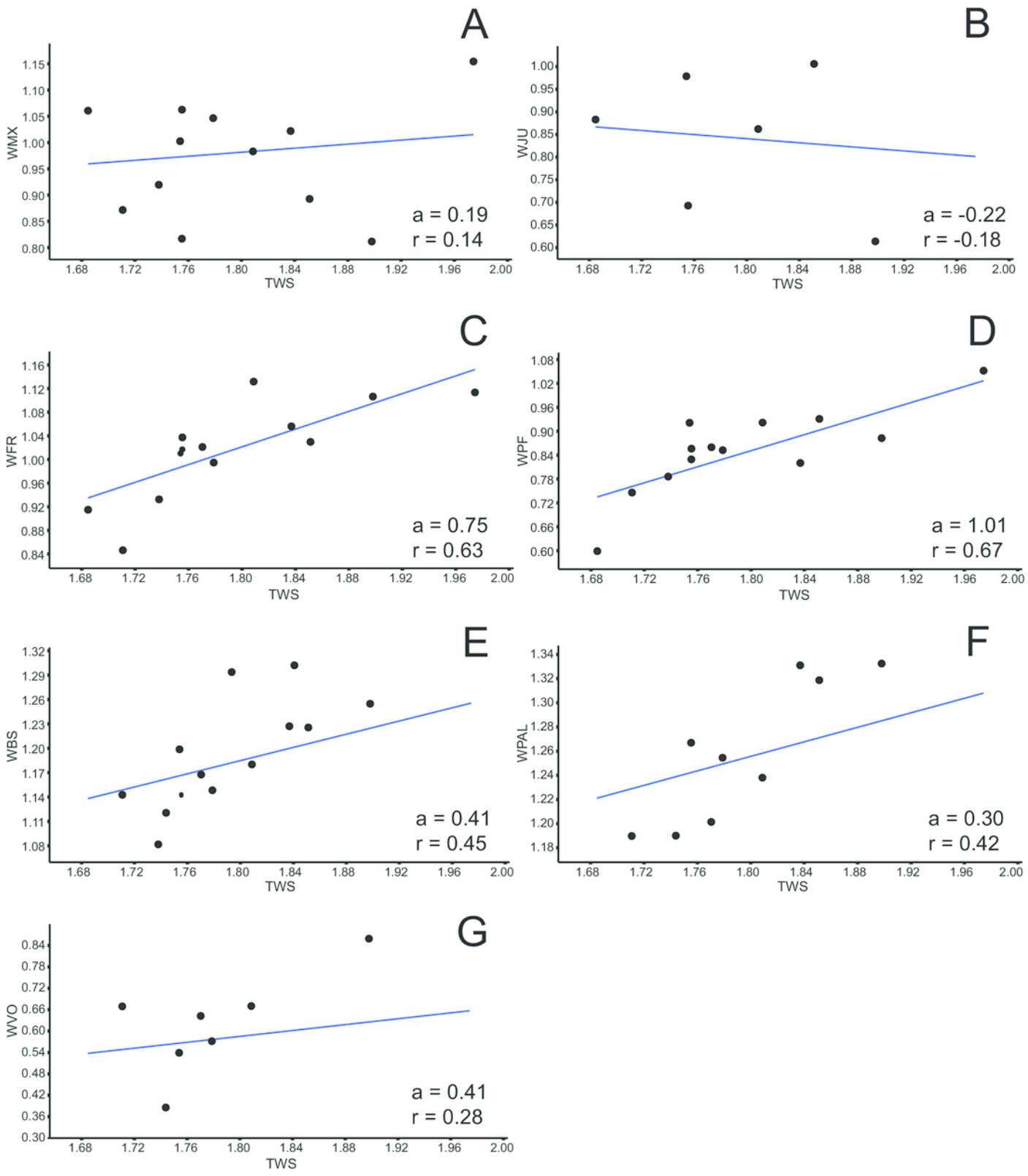
A
WMX
TWS
a = 0.19
r = 0.14
B
WJU
TWS
a = -0.22
r = -0.18
C
WFR
TWS
a = 0.75
r = 0.63
D
WPF
TWS
a = 1.01
r = 0.67
E
WBS
TWS
a = 0.41
r = 0.45
F
WPAL
TWS
a = 0.30
r = 0.42
G
WVO
TWS
a = 0.41
r = 0.28

6

PCA: raw data.

Principal Components Analysis (PCA) from raw data matrix using mean value substitution approach (A and B) and iterative imputation substitution approach (C) in replacing missing data. The 95% ellipse is given.

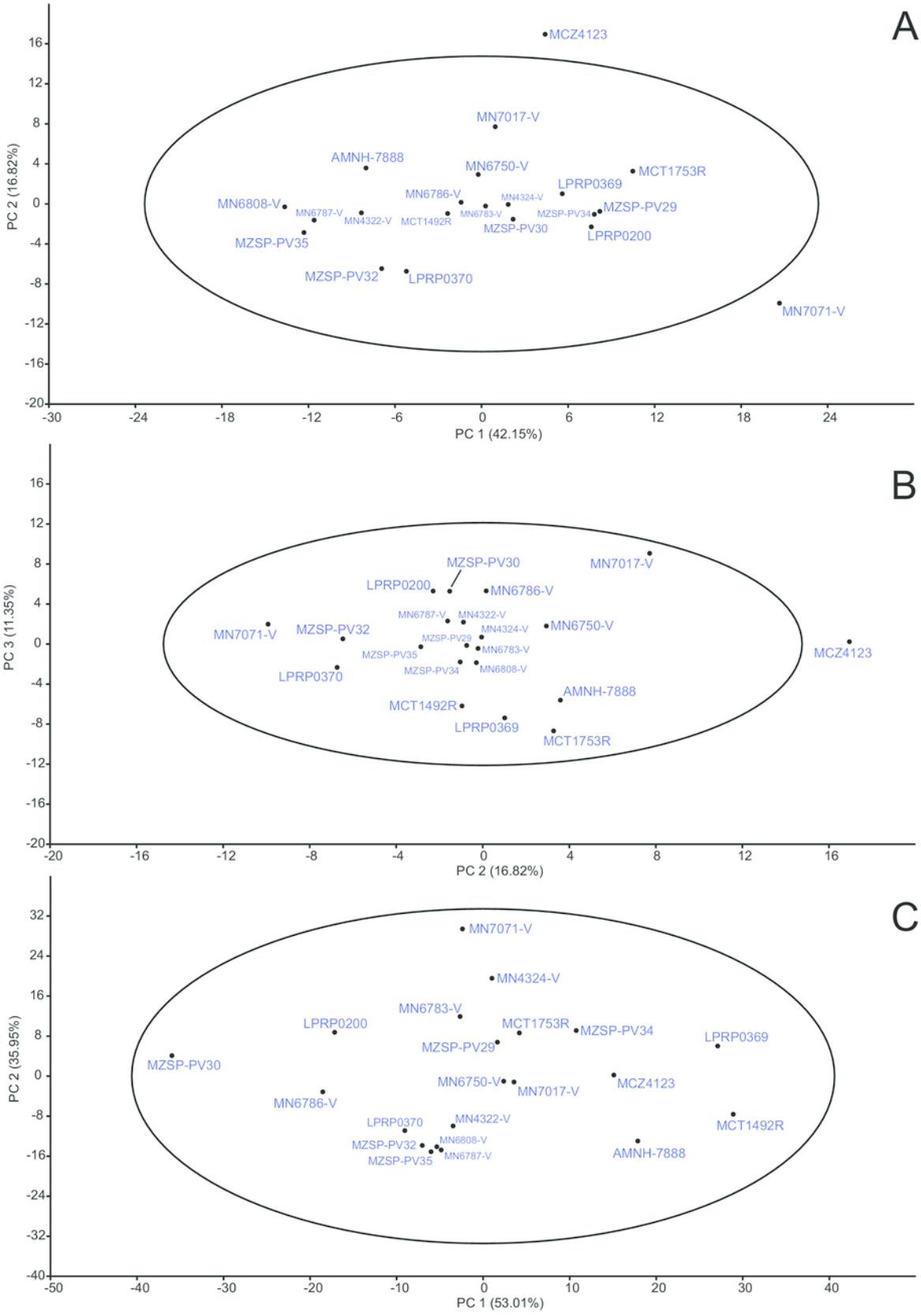
A
MCZ4123
MN7017-V
AMNH-7888
MN6750-V
MCT1753R
LPRP0369
MN6786-V
MN4324-V
MN6808-V
MN6787-V
MZSP-PV29
MN4322-V
MCT1492R
MN6783-V
MZSP-PV34
MZSP-PV30
LPRP0200
MZSP-PV35
MZSP-PV32
LPRP0370
MN7071-V
PC 2 (16.82%)
PC 1 (42.15%)
B
MZSP-PV30
MN7017-V
LPRP0200
MN6786-V
MN6787-V
MN4322-V
MN7071-V
MZSP-PV32
MN6750-V
MN4324-V
MZSP-PV29
MZSP-PV35
MN6783-V
MCZ4123
LPRP0370
MZSP-PV34
MN6808-V
AMNH-7888
MCT1492R
LPRP0369
MCT1753R
PC 3 (11.35%)
PC 2 (16.82%)
C
MN7071-V
MN4324-V
MN6783-V
LPRP0200
MCT1753R
MZSP-PV34
LPRP0369
MZSP-PV29
MZSP-PV30
MN6750-V
MCZ4123
MN7017-V
MN6786-V
MN4322-V
MCT1492R
LPRP0370
MN6808-V
MZSP-PV32
AMNH-7888
MZSP-PV35
MN6787-V
PC 2 (35.95%)
PC 1 (53.01%)

7

PCA: proportions data.

Principal Components Analysis (PCA) from proportions data matrix using mean value substitution approach (A) and iterative imputation substitution approach (B) in replacing missing data. The 95% ellipse is given.

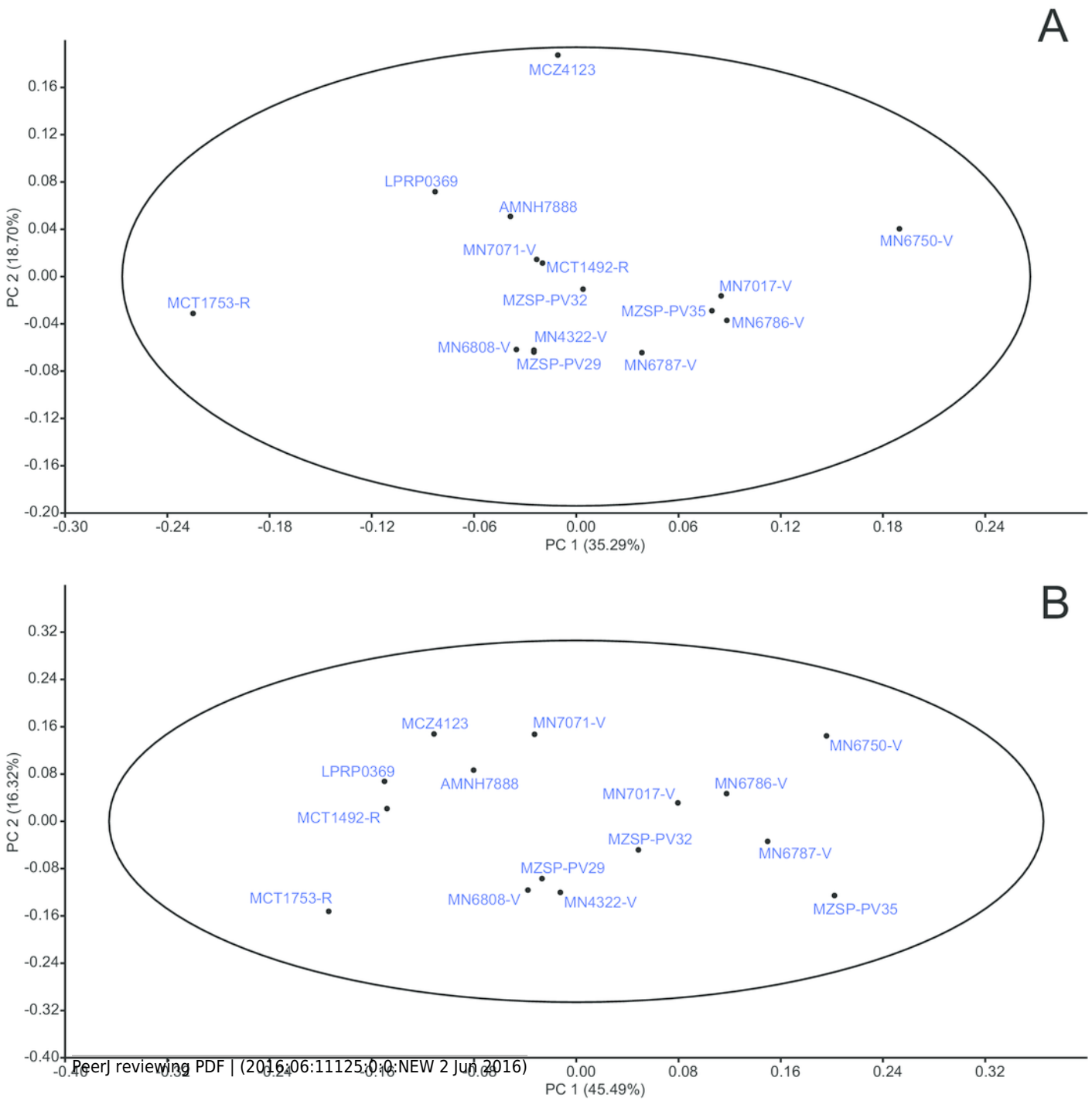

8

Evolution of PA-QJ contact and skull roofing in Podocnemidoidea.

Simplified phylogeny of Podocnemidoidea (Bothremydidae + Podocnemidinura) showing the evolution of the contact between parietal (green; PA) and quadratojugal (yellow; QJ), and its relation with the postorbital (red; PO) and skull roofing. Within Bothremydidae, both very emarginated (*Cearachelys placidoi*) and less emarginated (*Taphrosphys congolensis*) skulls are present, showing either no contact (*C. placidoi)* or contact present with small QJ (*T. congolensis*). Within Podocnemidinura, the contact PA-QJ is present and the skull roofing increased from a less roofed condition, found in *Brasilemys josai* and *Hamadachelys*, to a continuous increasingly growing well roofed condition within Podocnemididae, exemplified by *Bauruemys elegans*, *Lapparentemys vilavillensis* and *Podocnemis unifilis*, up to a fully roofed morphology in *Peltocephalus*. *Cearachelys placidoi* and *T. congolensis* modified from Gaffney et al. (2006); *Brasilemys josai* modified from Lapparent de Broin (2000); all others skulls modified from Gaffney et al. (2011).

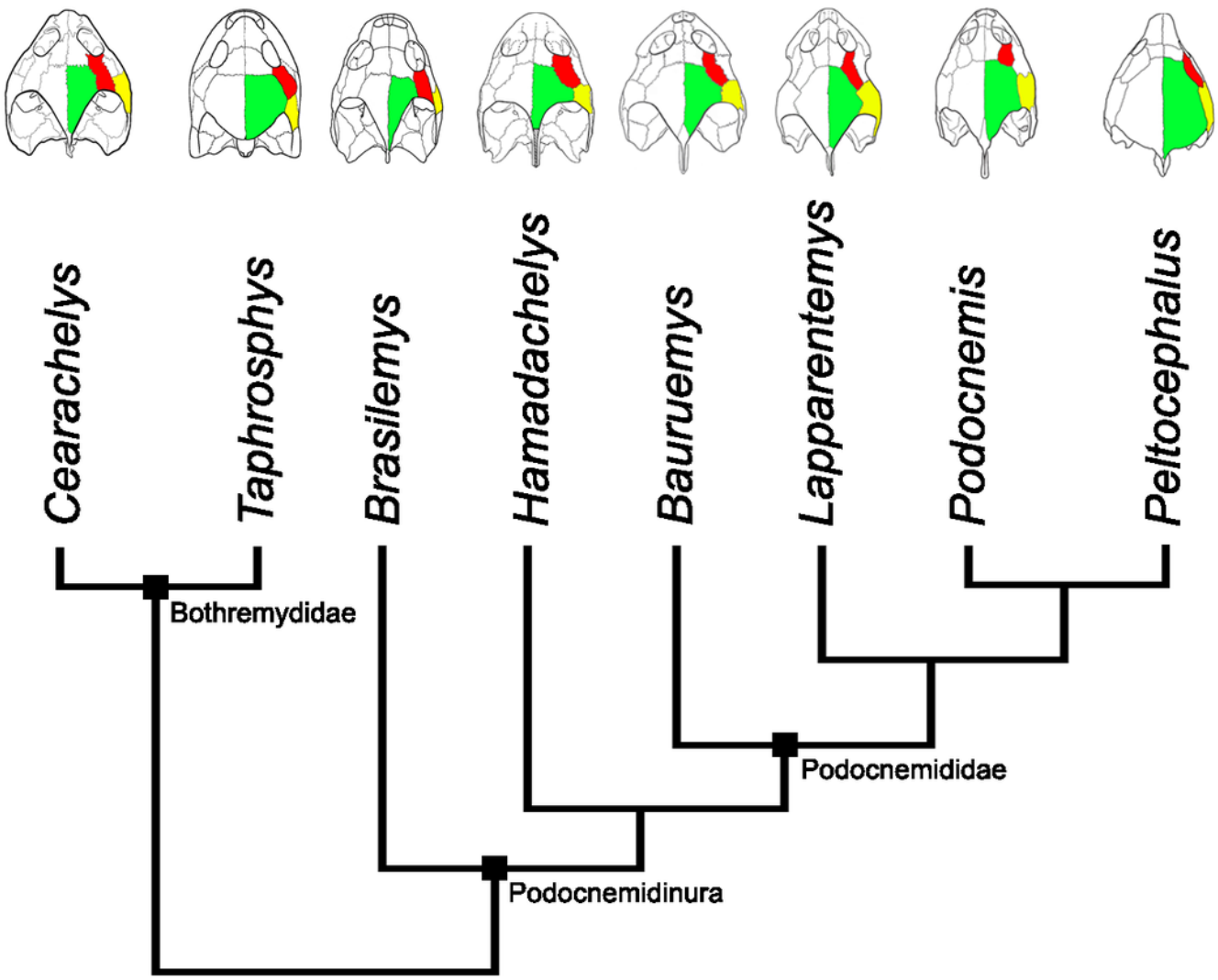
Cearachelys
Taphrosphys
Brasilemys
Hamadachelys
Bauruemys
Lapparentemys
Podocnemis
Peltocephalus
Bothremydidae
Podocnemididae
Podocnemidinura

Figure 9(on next page)

Sketch of jaw-closing muscles and its vector forces in *Podocnemis expansa*.

Dorsal (A and C) and left lateral (B and D) view of the skull of *Podocnemis expansa* (MZSP-0038) showing the muscle attachment places (A and B) and the direction vector forces (C and D) during jaw closing. The muscles and vectors of external adductor (green), posterior adductor (red), pterygoid muscle (blue), and *depressor mandibulae* (yellow) are sketched. Lenght and thickness of the arrows indicate the relative forces. **Abbreviations: art,** articular; **den,** dentary; **mx,** maxilla; **pa,** parietal; **ptp,** processus trochlearis pterygoidei; **qj,** quadratojugal; **qu,** quadrate; **so,** supraoccipital.

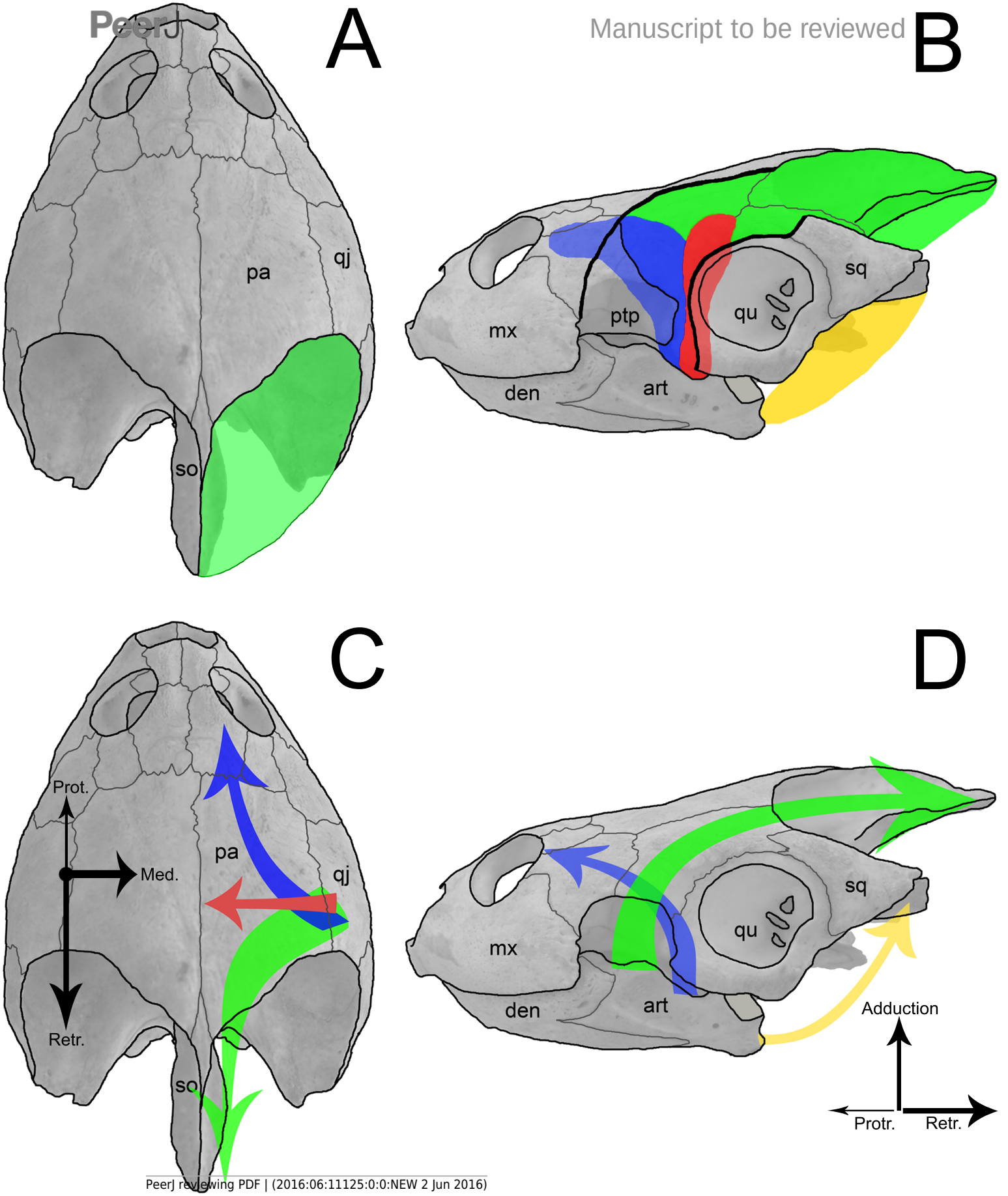
A
pa
qj
so
B
mx
ptp
qu
sq
den
art
C
Prot.
Med.
Retr.
pa
qj
so
D
mx
qu
sq
den
art
Adduction
Protr.
Retr.

Table 1(on next page)

ANOVA results for ImageJ and caliper comparisons.

Parameters calculated for each treatment of the ANOVA. The first three columns are relative to the caliper (cal). The three next are relative to the ImageJ (ImJ). The last column indicates the F values for each character. Measurements abbreviations: TLS, total lenght of the skull; TWS total width of the skull; LPF, lenght of prefrontal; WPF, width of prefrontal; LFR, lenght of frontal; WFR, width of frontal; LPA, lenght of parietal; WPA, width of parietal; SMX, stretch of maxilla; LVO, lenght of vomer; WVO, width of vomer; WCO, width of choannal; LPAL, lenght of palatine; WPAL, width of palatine; LPT, lenght of pterygoid; LBS, lenght of basisphenoid; WBS, width of basisphenoid; LBO, lenght of basisoccipital; LMX, lenght of maxilla; WMX, width of maxilla; LJU, lenght of jugal; WJU, width of jugal; LQJ, lenght of quadratojugal; WQJ, width of quadratojugal; LQU, lenght of quadrate; LPO, lenght of postorbital; WPO, width of postorbital; WOP, width of opisthotic; LSQ, lenght of squamosal.

Char.	N (Cal)	Mean (Cal)	σ (Cal)	N (ImJ)	Mean (ImJ)	σ (ImJ)	F value
TLS	8	63,72	10,87	8	62,26	11,36	0,069
TWS	9	60,42	9,45	8	64,83	13,58	0,617
LPF	9	9,78	1,26	9	8,05	1,80	5,617*
WPF	10	6,70	1,90	10	7,55	1,83	1,04
LFR	10	12,19	1,74	10	11,79	2,02	0,233
WFR	10	9,64	1,63	10	10,12	1,82	0,383
LPA	7	25,54	4,71	7	27,35	4,83	0,504
WPA	6	21,78	2,79	6	22,54	3,16	0,195
SMX	9	46,46	7,12	9	47,66	8,62	0,104
LVO	6	5,95	1,71	7	6,59	1,31	0,596
WVO	6	3,11	0,78	7	3,68	0,52	1,874
WCO	5	7,53	1,31	6	6,45	1,15	2,107
LPAL	7	8,26	1,25	8	7,21	2,81	0,828
WPAL	7	16,90	1,91	7	17,12	2,23	0,038
LPT	11	11,54	2,06	12	11,69	2,75	0,228
LBS	12	12,43	1,30	12	12,88	1,64	0,563
WBS	11	15,58	2,32	11	15,57	2,40	<0,001
LBO	7	13,00	1,84	7	13,84	1,85	0,726
LMX	10	24,28	4,20	9	19,22	4,15	6,937*
WMX	10	10,44	2,16	9	10,18	2,26	0,065
LJU	9	15,75	3,81	7	13,39	2,92	1,847
WJU	3	8,31	1,20	2	9,83	-**	2,709
LQJ	4	12,84	1,48	2	11,96	-**	0,366
WQJ	6	16,21	4,02	3	19,65	1,72	1,921
LQU	11	17,71	3,43	8	21,19	3,88	4,253
LPO	9	16,57	3,30	9	16,89	4,11	0,35
WPO	9	5,47	1,77	8	5,44	1,73	0,002
WOP	6	11,97	2,52	5	10,98	3,89	0,260
LSQ	5	10,63	3,28	4	12,26	3,86	0,467

1 Cal: caliper treatment. ImJ: ImageJ treatment. *significant statistically differences. **values not
2 calculated.

Table 2(on next page)

Descriptive statistics of all data.

Descriptive statistics of the three sorts of characters analyzed (total length and width, comprised measurements, and proportions of the measurements), including mean values (Mean), median values (Median), standard deviation values (SD), number of entries (N), and maximum and minimum values (Max-Min). All measurements are expressed in millimeters, except unscaled proportions between two measurements.

	Characters	Vector[a]	N	Mean	Median	SD	Min-Max
Total Length and Width	**TLS**	38-39	12	63.02	63.44	10.43	50.3-82.15
	TWS	-	15	63.08	58.93	11.91	48.39-94.27
Comprised measurements	**LPF**	1-4	15	8.35	8.31	1.69	4.35-10.94
	LFR	4-7	18	12.16	12.32	2.08	9.06-15.59
	LPA	7-12	12	28.88	27.36	6.45	20.54-43.80
	LVO	26-27	10	6.67	6.84	1.95	3.06-9.79
	LPAL	27-29	13	6.91	6.22	2.33	3.42-11.57
	LPT	29-30	19	11.72	11.94	2.42	6.95-17.99
	LBS	30-32	20	12.76	12.57	1.77	9.71-16.21
	LBO	32-38	13	14.16	13.38	2.12	11.13-18.28
	LMX	11-24	18	18.49	18.31	4.11	12.39-25.68
	LJU	10-14	14	12.42	12.32	3.28	4.46-17.22
	LQJ	13-18	6	11.15	10.66	2.38	8.26-14.45
	LQU	19-25	14	19.83	19.35	3.51	15.21-26.30
	LPO	6-13	17	17.54	15.72	4.12	11.51-24.59
	LSQ	20-21	11	11.71	11.08	3.07	8.24-16.57
	WPF	4-5	18	7.17	7.15	1.66	3.97-11.27
	WFR	7-8	18	10.55	10.61	1.88	7.02-13.55
	WPA	12-16	12	22.53	22.94	2.94	17.41-26.85
	SMX	11-11	15	47.85	46.35	7.63	39.24-66.10
	WVO	28-28	10	4.01	3.74	1.38	2.43-7.23
	WCO	28-34	9	7.00	6.61	1.39	5.23-9.10
	WPAL	29-35	14	18.08	18.23	2.37	15.24-21.50

	WBS	33-33	19	15.35	14.71	2.19	12.07-20.05
	WMX	10-11	16	9.80	9.84	2.24	6.48-14.27
	WJU	14-15	7	7.26	7.28	2.19	4.11-10.14
	WQJ	16-25	7	16.35	17.81	4.03	9.91-21.21
	WPO	13-14	16	5.15	5.00	1.83	2.73-9.05
	WOP	20-22	14	11.41	10.96	3.54	7.78-17.73
	CHARACTERS	**N**	**MEAN**		**MEDIAN**	**SD**	**MIN-MAX**
PROPORTIONS OF THE MEASUREMENTS	**LPF/TLS**	9	0.13		0.13	0.04	0.05-0.19
	LFR/TLS	11	0.19		0.18	0.02	0.17-0.22
	LPA/TLS	8	0.51		0.49	0.08	0.45-0.65
	LVO/TLS	8	0.11		0.12	0.03	0.06-0.15
	LPAL/TLS	10	0.11		0.11	0.03	0.06-0.17
	LPT/TLS	12	0.18		0.18	0.02	0.13-0.22
	LBS/TLS	12	0.21		0.21	0.02	0.17-0.24
	LBO/TLS	11	0.24		0.24	0.02	0.21-0.26
	LMX/TLS	11	0.29		0.28	0.06	0.17-0.38
	LJU/TLS	8	0.21		0.21	0.05	0.15-0.29
	LQJ/TLS	5	0.18		0.16	0.05	0.14-0.25
	LQU/TLS	10	0.30		0.30	0.04	0.23-0.37
	LPO/TLS	11	0.29		0.29	0.03	0.23-0.35
	LSQ/TLS	7	0.19		0.20	0.05	0.12-0.24
	WPF/TWS	13	0.12		0.12	0.02	0.08-0.15
	WFR/TWS	13	0.17		0.17	0.02	0.14-0.21
	WPA/TWS	10	0.37		0.37	0.05	0.29-0.44

SMX/TWS	12	0.75	0.76	0.06	0.67-0.86
WVO/TWS	7	0.09	0.07	0.02	0.04-0.09
WCO/TWS	7	0.11	0.12	0.02	0.09-0.13
WPAL/TWS	9	0.29	0.29	0.02	0.27-0.32
WBS/TWS	12	0.24	0.24	0.02	0.22-0.28
WMX/TWS	12	0.16	0.15	0.04	0.08-0.24
WJU/TWS	6	0.12	0.13	0.05	0.05-0.17
WQJ/TWS	7	0.29	0.30	0.08	0.16-0.37
WPO/TWS	12	0.08	0.08	0.02	0.06-0.13
WOP/TWS	11	0.18	0.17	0.04	0.13-0.23

SD: standard deviation values. N: number of entries. Max-Min: maximum and minimum values.
[a] straight line between two landmarks used to trace linear measurements (see figure 2 to visualize the landmarks).

Table 3(on next page)

PCA loadings: raw data.

Loading values of characters in the raw data matrix related to the first three principal components in PCA, comparing the Mean Value (mv) approach with the Iterative Imputation (ii) approach.

Char.	PC1 (mv)	PC2 (mv)	PC3 (mv)	PC1 (ii)	PC2 (ii)	PC3 (ii)
LPF	-0.05	0.04	0.02	-0.04	-0.05	-0.05
WPF	0.14	0.02	0.05	-0.001	0.12	0.08
LFR	0.19	-0.01	-0.09	0.02	0.14	-0.04
WFR	0.17	0.10	-0.02	0.01	0.13	-0.001
LPA	0.27	0.74	0.10	0.89	0.04	0.11
WPA	0.12	0.17	-0.01	0.22	0.16	0.06
SMX	0.66	-0.45	-0.22	0.01	0.59	-0.34
LVO	0.05	0.07	0.03	-0.02	0.11	0.01
WVO	0.04	0.03	-0.07	0.02	0.09	-0.11
WCO	0.05	0.04	-0.07	0.03	0.12	-0.08
LPAL	0.08	0.04	0.06	0.04	0.13	0.27
WPAL	0.15	0.02	-0.09	0.03	0.23	-0.05
LPT	0.17	-0.14	0.08	-0.02	0.13	0.10
LBS	0.14	-0.02	0.01	0.01	0.10	0.05
WBS	0.12	0.05	-0.07	0.02	0.19	-0.05
LBO	0.11	0.11	-0.07	0.03	0.20	0.03
LMX	0.18	-0.17	0.68	-0.18	0.16	0.38
WMX	0.09	-0.07	0.25	-0.08	0.11	0.19
LJU	0.08	0.13	0.30	-0.14	0.19	0.25
WJU	-0.01	0.02	0.10	0.01	-0.01	0.21
LQJ	0.04	-0.05	-0.04	-0.16	0.18	-0.11
WQJ	0.03	0.07	0.29	-0.11	0.17	0.42
LQU	0.18	-0.13	0.32	-0.13	0.21	0.18
LPO	0.36	0.19	-0.13	0.03	0.29	0.02
WPO	0.11	-0.04	0.05	-0.01	0.10	0.04
WOP	0.21	0.15	-0.23	0.06	0.30	-0.24
LSQ	0.07	0.19	0.11	0.16	0.02	0.43

1 Char: characters. mv: Mean Value approach. ii: Iterative Imputation approach.

Table 4(on next page)

PCA loadings: proportion data.

Loading values of characters in the proportions data matrix related to the first two principal components in PCA, comparing the Mean Value (mv) approach with the Iterative Imputation (ii) approach.

Char.	PC1 (mv)	PC2 (mv)	PC1 (ii)	PC2 (ii)
LPF/TLS	0.003	-0.13	0.11	-0.30
LFR/TLS	0.001	-0.04	0.03	-0.02
LPA/TLS	0.28	0.66	-0.13	0.67
LVO/TLS	-0.002	0.05	-0.03	-0.02
LPAL/TLS	0.08	0.02	0.07	0.12
LPT/TLS	-0.05	-0.10	-0.02	-0.01
LBS/TLS	0.03	-0.17	0.11	-0.10
LBO/TLS	-0.02	-0.04	0.01	-0.04
LMX/TLS	0.38	-0.43	0.48	-0.18
LJU/TLS	0.16	0.01	0.16	0.14
LQJ/TLS	0.06	-0.09	0.21	-0.17
LQU/TLS	0.27	-0.07	0.28	0.05
LPO/TLS	-0.16	0.13	-0.18	0.03
LSQ/TLS	0.16	0.23	0.20	0.34
WPF/TWS	0.07	0.09	-0.001	0.11
WFR/TWS	0.07	0.13	0.02	0.05
WPA/TWS	0.23	0.32	0.08	0.33
SMX/TWS	0.38	-0.12	0.33	-0.01
WVO/TWS	-0.05	-0.04	-0.04	-0.10
WCO/TWS	-0.04	0.07	-0.11	0.04
WPAL/TWS	0.04	-0.07	0.04	-0.003
WBS/TWS	0.03	-0.05	0.02	-0.03
WMX/TWS	0.35	-0.05	0.30	0.03
WJU/TWS	0.18	0.01	0.26	0.19
WQJ/TWS	0.48	-0.003	0.41	0.20
WPO/TWS	0.02	0.01	-0.01	0.07
WOP/TWS	-0.13	0.27	-0.21	0.09

1 Char: characters. mv: Mean Value approach. ii: Iterative Imputation approach.